Assessment of the natural variability of cob buildings hygric and thermal properties at material scale: Influence of plants add-ons

Junior Tchiotsop, Nabil Issaadi, Philippe Poullain, Stéphanie Bonnet, Rafik Belarbi

ASSESSMENT OF THE NATURAL VARIABILITY OF COB BUILDINGS HYGRIC AND THERMAL PROPERTIES AT THE MATERIAL SCALE: INFLUENCE OF ADD-ONS

Junior Tchiotsop[1,2,3], **Nabil Issaadi**[*1,2], **Philippe Poullain**[1,2], **Stéphanie Bonnet**[1,2], and **Rafik Belarbi**[4]

[1] GeM CNRS UMR 6183, Nantes université, 44600 Saint-Nazaire Cedex 1, France.
[2] IRSTV, CNRS FR2488, Ecole Centrale de Nantes, 44300 Nantes, France.
[3] ADEME, BP 90406 49004 Angers Cedex 01 France
[4] LaSIE, UMR CNRS 7356, Université la Rochelle, 17042 La Rochelle Cedex 1, France.

Abstract

This paper takes place in improving the energy performance assessment of cob buildings, by evaluating the variability of its hygrothermal properties at the material scale, related to the traditional construction process. For so, we proposed and analysed data to handle the variability of the hygrothermal properties. The specimens were manufactured using a moulding method representative of on-site cob wall manufacturing process, for three plants species (hemp shiv, flax yarn and hay stalk) and three fibre content (0, 1% and 3%). Using non-destructive tests and statistical analysis, the random variability of cob composites hygrothermal properties (density, thermal conductivity, specific heat capacity, water-vapor permeability, moisture buffering value and sorption isotherms) was found as well as the variability distribution. It has been shown that the variability of properties is sensitive to the nature of plant fibres specie and the fibre content. Using the variability indicators, it has been found on thermal conductivity, a low coefficient of variation of 2.88% for 1%-flax fibred mixture (lower than unfibred material) and a high one for 3%-hemp composites of 10.88%. The variability of sorption isotherms was usually found to be high at lower humidity loads. It has been shown that increase fibre[1] content stabilizes the variability of properties. Moreover, some evolution trends of the variability according to mixes was proposed; two parameters were found: the first, either FC^{max} highlighting the fibre content for which the maximum of variability was achieved or FC^{min} for the opposite; the second is FC^{res} highlighting the residual variability, for high fibre content. The distribution of properties were found to be generally centered.

Keywords: variability assessment, cob material, density, thermal conductivity, specific heat capacity, Water vapor permeability, Sorption isotherms, Moisture buffering value.

Nomenclature

IR:	Interquartile Range	CV:	Coefficient of variation
CVm:	Model CV	CV:	Experimental CV
FC:	Fibre content	MBV $(g/m^2.RH)$:	Moisture Buffering Value
V_{tot} :	Total variance	V_{int} :	Intrinsic variance
MIP:	Mercury Intrusion Porosimetry	SSS:	Saturated Salt Solution method
DM(s):	Distribution Model(s)	PDF:	Probability Density Function
m:	Expectation	s:	Standard deviation
μ, σ, k, λ:	PDF models parameters	k_m:	Water vapour permeability
λ $(W/m.K)$:	Thermal conductivity	$\rho.C_p$ $(MJ/m^3.K)$:	Specific Heat Capacity

*Corresponding author, E-mail : nabil.issaadi@univ-nantes.fr
[1] to make reading easier, we named as "**fibre**" on this paper, hemp shiv and hay stalk aggregates.

1. Introduction

It is now proven that planet Earth is suffering Global Warming effects with a mean surface temperature that increases, evaluated between 0.45°C and 0.53°C each 100 years [1,2]. In 2019, the dwellings construction has been responsible for 38% of greenhouse gases emissions and for 35% of the overall energy consumption worldwide [3]. This is due to several factors such as the lack of resources for construction inducing long distance transportation and thus pollution, to material manufacturing – especially cement that provides around 0.8 ton of CO2 per ton of produced cement – to the modern construction techniques that are energy consuming [4, 5] and to the overall energy consumption to ensure hygrothermal comfort inside the buildings.

In this context, raw earth could help address the main issues of global warming in the construction sector: energy and natural resources savings. Indeed, raw earth exhibits many advantages:

- it is generally available locally and thus requires little transportation;
- it can be used in low-tech solutions with little transformations and is recyclable;
- the construction techniques involving raw earth require little mechanization;
- earthen buildings have a better thermal inertia than conventional buildings and earth is acertained as a good hygric regulator [6, 7]

Earthen buildings are built using different techniques depending on the local climate and earth composition, on the local skills of craftsmen or habits. In France, most of these techniques are met such as adobe bricks, rammed earth, cob or compressed earth bricks [8, 9]. However, assessing the true performances of earthen buildings regarding the energy consumption is still a research issue since it has been demonstrated that the heating or cooling energy consumptions of these buildings are lower than those predicted by conventional heat transfer models [10]. This is due to the fact that:

- the coupling between heat and moisture transfer is neglected in these models;
- the hygrothermal properties of earthen materials are subject to strong variabilities relative to the technique, the earth composition, etc.

One research issue is thus to measure reliable properties for earthen materials and especially cob. Contrary to conventional construction techniques, cob does not comes under any standards or regulations, even if, in France, rules have recently been established by practitioners (craftsmen, architects, engineers, researchers...) for most techniques [11] in order to incentivise them to converge towards common construction rules. Nevertheless, differences will remain in the properties and behaviours between different cob buildings because:

- the techniques slightly differ from one project to another;
- the type of plant is chosen according to the local availability of vegetable resources;
- the fabrication process of a cob wall consists in stacking earth clods which can yield to local heterogeneity in the material (joints between clods).

All these reasons are sources of global (between different projects) or local (inside a given wall) property variability. However, other reasons may explain variability in the value of a given material property. Baescher et al. [12] classify them into three groups:

- **the variability linked to the limited knowledge:** measurement technique, prediction models and hypotheses, constitutive relationship, etc.
- **the variability linked to decision-makers:** that could be improved.
- **the natural variability:** not controllable by the operator, the one investigated by this study. Indeed, assuming a variability measured as natural and even better as random process permits to use the probability theory and thus statistical tools.

Therefore, the experimental value of a given property is the sum of a deterministic term and a variable term [13–15].

- **the deterministic term:** (also called accepted value in NF ISO 5725-4:2020 standard [15]): it is generally the average value of a parameter, assumed to be representative. For correlated series of data, there could be an existing error on this latter related to the deterministic model used [16].
- **the variable term**: it is the sum of all the sources of variability. For quality control of products, Shewhart [17] assumes both as one variability and assigns the random variability to the cumulative effect of several minor factors [17]. For earthen material for example, it can be the sum of the differences in porosity textures, fibers distribution, orientation and clustering, organic matter content from one specimen/wall position to another.

Many works have been carried out about the variability of the hygrothermal and mechanical properties of geo-based and bio-based materials. It has been shown that earthen materials properties are sensitive to the extraction site [18, 19], to the testing protocol [18–20], to the add-ons [21–25] and to the inter laboratory test conditions [20, 26]. Table 1 summarizes the random variability (measurement uncertainties) performed on different mixtures of cob materials in the literature, using the coefficient of variation (CV). The intrinsic, repeatability and reproductibility uncertainties were listed or computed, even for a low number of specimens. The first one is the natural variability: tests are performed on specimens from the same batch and different sources of uncertainties are removed. For the second, the tests are performed on one specimen and the third includes external uncertainties such as the change of the protocol, the device, the laboratory, the operator, etc.

Across the papers listed, the material uncertainty for the density (ρ) of unfibred materials does not exceed 2%; while, it can reach 17% for lightweight materials [27]. By using a higher number of specimens, there is an increase in the measurement uncertainty; Barnaure et al [28] found an uncertainty as high as 4% on the material density and 10% for the thermal conductivity for 18 specimens. Moreover, the uncertainty evolves according to the plant add-ons used [24] as well as to their size [29]. The variability of the properties can be also sensitive to the compaction load direction during specimen manufacturing. Maillard and Aubert [30] found lower uncertainty on the thermal conductivity and water-vapor permeability for specimens cored in a parallel direction to compaction. The material uncertainty is also linked to the measurement method as shown by Cagnon et al [31] on thermal conductivity measurements: higher variability is found using the Desprotherm device than the Guarded Hot Plate one (25% vs 19% respectively).

Research works have also been performed to assess the effects of the variability of the hygrothermal properties of the geo-based and bio-based materials as well as their impact on the transfer kinetics of house walls [32] and on energy performance of buildings [33, 34]. The effects are not always negligible; Andrianandraina et al [34] have made a sensitivity analysis of the Kunzel coupled heat and mass transfer model inputs (including climate) for lime-hemp concrete. They found that the thermal conductivity variability have an influence of 38% on the yearly heating energy consumption of a building equivalent to 348 kWh/m².year.

We propose in this work to promote and add value to cob buildings heritage by giving more reliability on this type of construction. In contrast to rammed earth buildings where compaction energy is well defined and can be handled on the site and at laboratory scale, cob building is actually a man-made construction with earth mix in a plastic state. There is a need to handle cob specimen fabrication, especially this man-made side of construction process. By the way, we proposed a moulding method of cob specimens and the estimation of the hygrothermal properties random variability. The effects of add-on plant specie (hemp shiv, flax yarn and hay stalk) and substitution rates will be evaluated. Firstly, the variability of the properties will be assessed; meanwhile, data processing for thermal properties will be done to get the effects of uncontrolled protocol steps on the total variability (to get the intrinsic variability). Secondly, we will propose some probability distribution functions of mixes as input values for the reliability of energy performance assessment of cob buildings. And finally, the variability data will be grouped to propose a close discussion on the evolution of the variability according to the fibre content of mixtures.

Table 1: Uncertainty of cob/adobe materials. NS: Number of specimens, A_{cap}: Capillary absorption coefficient, w_{cap}: capillary water content; ρ: density, ϕ: porosity; μ_d: Resistance to water vapour diffusion for dry cup test; μ_w: Resistance to water vapour diffusion for wet cup test, HD (Hotdisk), Cal (Calorimeter), DES (Desprotherm), GHP (Guarded Hot Plate)

Reference	**Material**	**Building type**	**Material uncertainty (%)**	**Repeatability uncertainty (%)**	**Reproductibility uncertainty (%)**
Feng et al, 2015 [35]	Autoclaved aerated concrete	Concrete building	**NS: 3-5**	**NS: 2-26**	**NS: 2-26**
			A_{cap} : 7	A_{cap} : 8	A_{cap} : –
			w_{cap} : 4	w_{cap} : 2	w_{cap} : 11
			ρ: 1	ρ: 0	ρ: -
			ϕ: 0	ϕ: 0	ϕ: 2
			μ_d: 6	μ_d: 6	μ_d: 19
			μ_w: 4	μ_w: 1	μ_w: -
	Calcium Silicate Board	Used for water-proofing and surface adjustment	A_{cap} : 0	A_{cap} : 2	A_{cap} : 4
			w_{cap} : 1	w_{cap} : 0	w_{cap} : 3
			ρ: 0	ρ: 0	ρ: 1
			ϕ: -	ϕ: 0	ϕ: 1
			μ_d: -	μ_d: 2	μ_d: 20
			μ_w: 1	μ_w: 3	μ_w: 42
	Ceramic brick	Fired earth brick buildings	A_{cap} : 15	A_{cap} : 2	A_{cap} : 15
			w_{cap} : 4	w_{cap} : 0	w_{cap} : 7
			ρ: 1	ρ: 0	ρ: 1
			ϕ: 4	ϕ: 0	ϕ: -
			μ_d: 17	μ_d: 2	μ_d: 45
			μ_w: 17	μ_w: 4	μ_w: -
H. Cagnon et al, 2014 [31]	Extruded earthen bricks accross Occitanie region, France	Adobe/cob	**NS: 5**	x	x
			ρ: 0-2	x	x
			λ GHP: 1-19	x	x
			λ DES: 8-25	x	x
			μ_d: 0-24	x	x
			μ_w: 1-21	x	x
Medjelek et al, 2016 [7]	Unfired earth bricks	Adobe/cob	**NS: 3**	x	x
			ρ: 1	x	x
			λ HD: 10	x	x
			C_pCal : 5	x	x
Labat et al, 2016 [36]	Straw-clay	Adobe/cob	**NS: 3**	x	x
			ρ: 1-17	x	x
			λ HD: 3	x	x
			C_p Cal: 6	x	x
			μ_d: 12	x	x
			μ_w: 15	x	x
Fgaier et al, 2016 [27]	Straw-clay	Adobe/cob	**NS: 3**	x	x
			ρ: 1-17	x	x
			λ HD: 3	x	x
			μ_d: 12	x	x

			μ_w: 15	x	x
Maillard et Aubert, 2015 [30]	Extruded earthen bricks parrallel to compaction direction (//) and perpendicular (P)	Adobe/cob	**NS: 3**	x	x
			λ GHP (//): 2-9	x	x
			λ GHP (P): 6-14	x	x
			μ_d (//): 5-11	x	x
			μ_d (P): 1-8	x	x
Gandia et al, 2019 [37]	Adobe bricks	Adobe/cob	**NS: 5**	x	x
			ρ: 1	x	x
			A: 82	x	x
			A_{cap} : 24	x	x
	Adobe bricks with reinforced glass fibers polymers (10% substitution rate)	Adobe/cob	**NS: 5**	x	x
			ρ: 2	x	x
			A: 3	x	x
			A_{cap} : 9	x	x
Ashour et al, 2010 [24]	Unfibred soil	Adobe/cob	**NS: 3**	x	x
			ρ: 2	x	x
	soil + barley straw (7,5%)	Adobe/cob	ρ: 2	x	x
	soil + wheat straw (7,5%)	Adobe/cob	ρ: 5	x	x
	soil + wood shavings (7,5%)	Adobe/cob	ρ: 3	x	x
Barnaure et al, 2021 [28]	Unfibred cob material	Adobe/cob	**NS: 18**	**NS: 20**	x
			ρ: 4	ρ: x	x
			λ HD: 10	λ HD: 5	x
	8% fibred cob material	Adobe/cob	ρ: 4	ρ: x	x
			λ HD: 12	λ HD: 4	x

2. Materials and methods

2.1. Materials

The soil is an excavation waste coming from the ecological district “Maison Neuve” of Guérande, France. Figure 1a shows the particle size distribution of the soil found in accordance with the NF EN ISO 17892-4:2018 standard [38]. The soil is a sandy-loam made up of 8% clay, 47% silt and 45% sand. The classification of the soil, based on the French soil science organisation “GEPPA” is presented on figure 1b. It has to be noted that in the GEPPA diagram [39], the upper dimension of the silt is 50 μm, different from the one considered in NF EN ISO 17892-4:2018 standard, such that based on this system the silt content is 44%, while the sand content is 48%. On the texture diagram, the grey areas are mentioned by Rojat et al. [40] as generally considered suitable for rammed earth and the green dots are values obtained from samples extracted from existing rammed earth houses. The green zones correspond to the textures observed by Hamard et al [41] on cob techniques in Brittany. The Atterberg limits were determined based on NF EN ISO 17892-12:2018 [42]. The plastic limit is $W_P = 17\%$, while the liquid limit is $W_L = 34\%$. The value of the plasticity index is $IP = 17$ and thus is moderately plastic according to the LCPC soil classification [43]. The Methylene blue value is 1.9 and was determined based on NF EN 933-9+A1:2013 standard [44]. According to Dakshanamurthy and Raman [45], Turköz and Tosun [46] classifications, the soil has little swelling.

The variability has been studied for hemp shiv, flax yarn and hay stalk with fibre[2] contents of 1% and 3% of the dry soil mass.

Hemp shiv is manufactured by CHANVRIBAT company and is already calibrated. It is the woody part (bark) of stems of the hemp plants. They have a bulk density of 100-110 kg/m^3, a particle skeleton density ranging between 1140 and 1460 kg/m^3 according to the measurement method and the graininess [47]. Hemp shiv show a mean length of 40 mm (sieve size of 50% of passing by weight) and a mean aspect ratio of length over width of 4 [48].

Flax yarn are extracted fibre from flax stalk cells. They are used in textile industry or for plumbing sealing, and are provided as wire rolls. They are obtained after a scutching and a combing process. It shows a high intrinsic characteristics variability - a thinner diameter ranging from 13 to 80 m, a particle skeleton density between 1380 and 1550 kg/m^3 by mean and high tensile strength of 600-2000 MPa across many species [49–51]. They were cut to 50 mm length.

As third add-on, dry hay stalk were used. By the way, they are made up of the stem and the leaves of the hay plant. They are even used to feed animals or as litter for domesticated rabbits. We found diameter of stem ranging from 0.13 mm to 1.27 mm and they were cut to 50 mm length too. Lisowski et al [52] found a particle skeleton density of 1102 kg/m^3 and a dry bulk density of 514 kg/m^3

Figure 2 shows the microscopic scale observations of unfibred and 1% fibre content mixtures. WF specimen looks like a porous stone, with a high frequency of pores. For flax yarn/earth composites, a high concentration of fibre can be seen and the fibres are well dispersed through the composite with an easy fit into the earth matrix. The hay stem and leaves separates during mixing operation; a lack of bonds of the fibre with earth matrix is more pronounced. For hemp composites, large pores can be observed like in the material without fibres. Moreover, the interface between hemp shives and the matrix does not show the high porosity seen in the hay/earth composites.

Figure 3 shows the differential distribution curve and the cumulative distribution curve of materials. For 1% fibred mixes, the modal porosity is approximately at the same diameter ($2\mu m$); that means that the earth matrix is always well represented in mixes. Whilst, Ha-3% specimens have a fairly uniform distribution, highlighting many pores textures representation. This could to an increasing of the variability of properties with fibre content.

2.2. Methods

In order to clearly present the different steps followed in the framework of this work, a brief work plan is done on the figure 4.

First, materials were manufactured following the protocol described at section 2.2.1, representing the onsite assembly of the cob walls. Second, tests were carried out on different specimens from the same batch and the total variability was described, by using the four quartiles and mean values (Black scatter in Tuckey diagram) [53], the interquartile range and the coefficient of variation. Data that did not fall into the 99.3% confidence interval of the normal law were assumed as outliers.

Third, an approximation of the probability density function of properties was proposed, based on three distribution models (DMs). The parameters of the PDFs were found based on the maximum log-likelihood estimation and a sensitivity analysis was conducted on the number of Bins-Clustering (BC) of the experimental distribution. Finally, a discussion will be done on the evolution trends of the variability of cob materials properties with fibre content.

2.2.1. Specimen preparation and curing

The soil was wetted 24 hours prior to fabrication in order to ease the mixing operation and to avoid clay lumps formation. The water content was determined by drying some specimens in order to adjust the amount of water necessary to reach the prescribed water content (**19%**). Plants add-ons were pre-wetted for 10 min and wrung out. In one sense, this limited the formulation variability between mixes by achieving a uniform plastic consistency and preventing the absorption of clay hydration water by the fibres. In another sense, this allowed to limit fibre breakage. The mixtures nomenclatures and designs are given in table 2. We proposed also a volume fibre content

[2]to make reading easier, we named as "**fibre**" on this paper, hemp shiv and hay stalk aggregates.

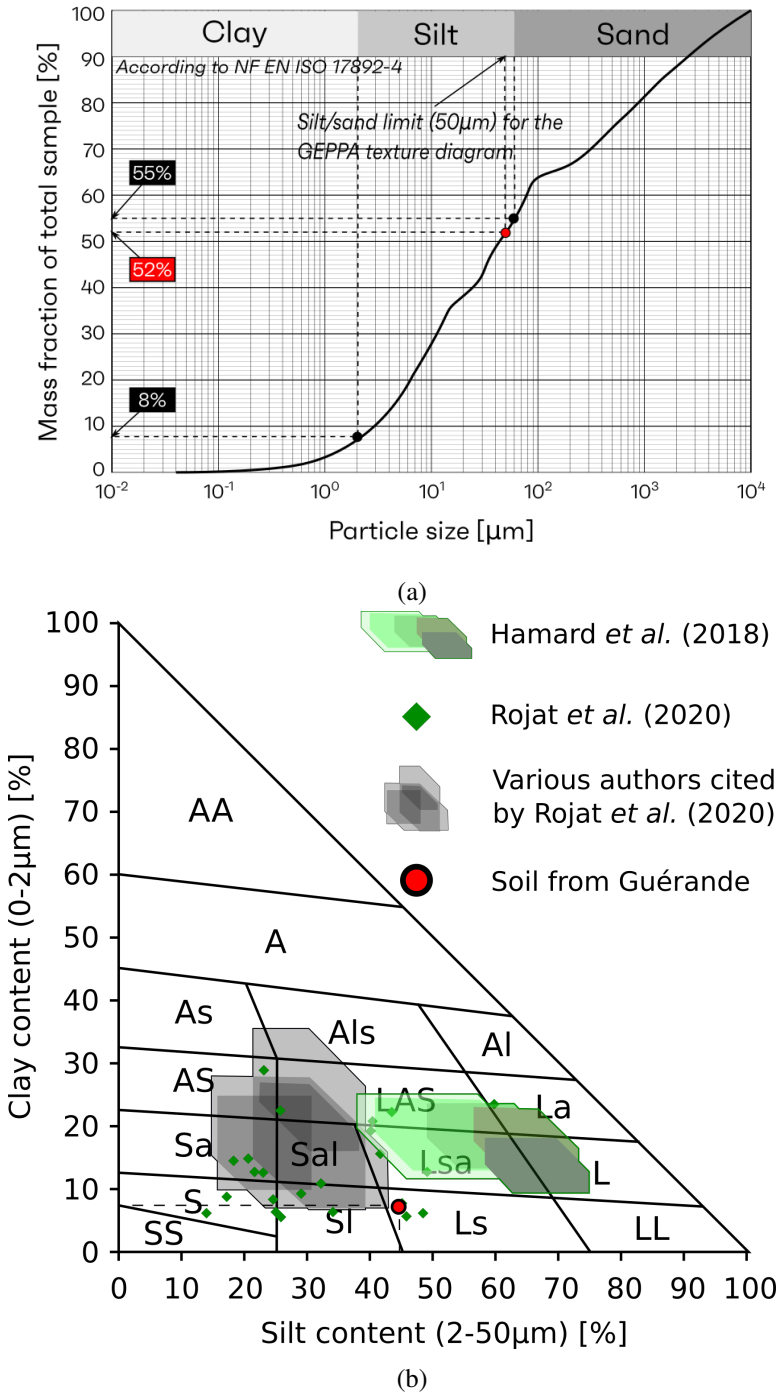

Figure 1: Particle size distribution of the soil (a) and ”GEPPA” classification of the soil (b) [28]

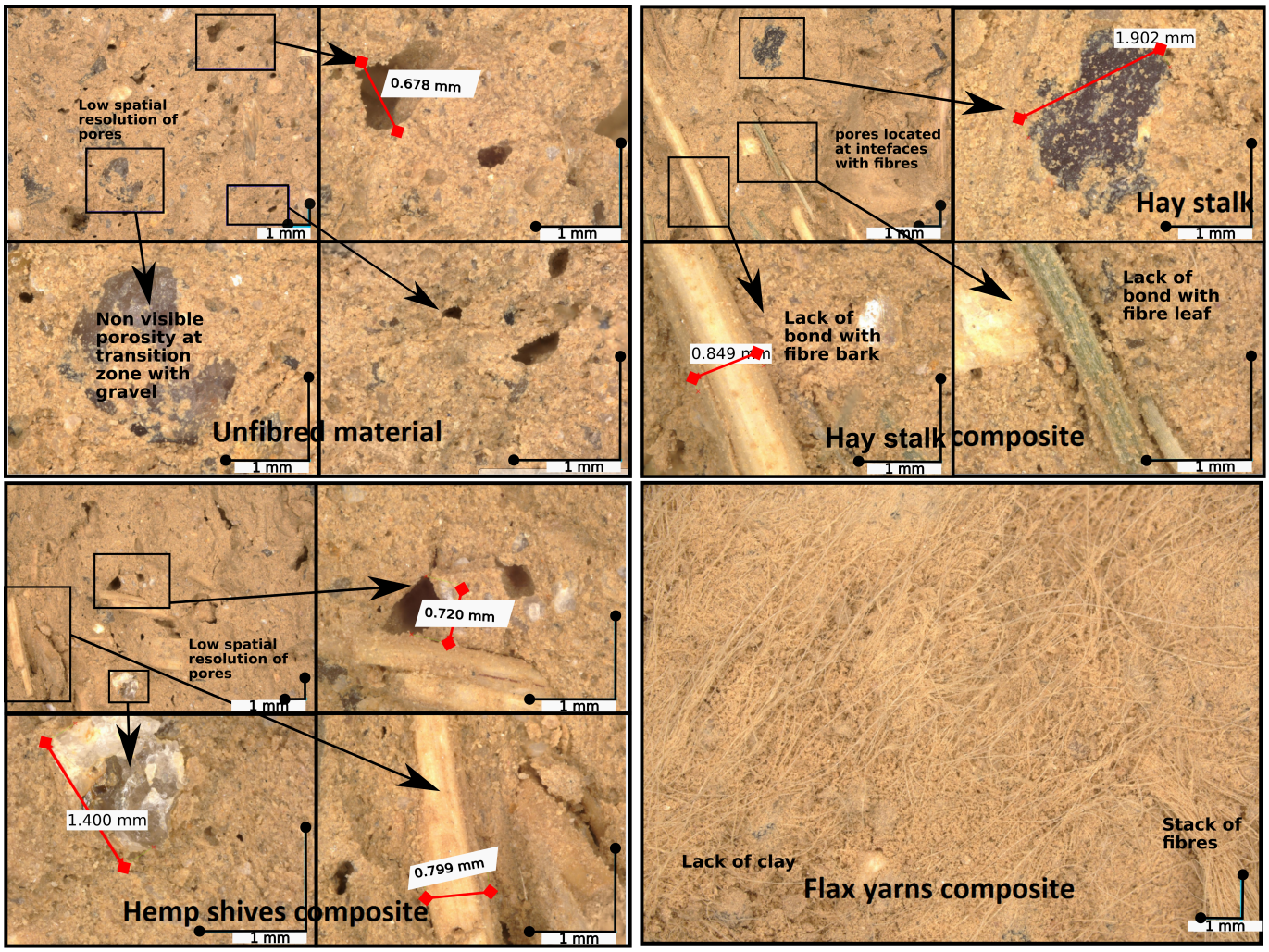

Figure 2: Digital microscope observations of unfibred and 1% fibre content mixes

per m^3 of soil and dry material, knowing the fibres mass density, the soil one (2650 kg/m^3) and the dry soil density (from specimens). Therefore, the volumes FC takes into consideration the variability of pores across specimens.

The fresh mixes were kneaded in a mixer for 20 minutes with at least 3 pauses for manual stirring, to get a randomly distributed fibres and a homogeneous water content. Materials were cast in 40x40x160 mm^3 steel moulds to obtain specimens for the thermal properties measurements; ϕ110x25 mm PVC moulds were used to produce specimens for water vapour permeability tests; ϕ110x40 mm PVC moulds were used to make specimens for the Moisture Buffering Value (MBV) measurements; 10x10x10 mm^3 and 50x50x20 mm^3 size specimens were used for sorption isotherms with ProUmid and Saturated Salt Solutions boxes devices respectively. The moulding of cob material at the laboratory scale was done following some authors process [54, 55]. The material was thrown in the mould with a strong impact and manually pressed in order to get a certain degree of uncontrolled compaction, to reproduce the on-site procedure with human feet treading in shallow pits. This was done for two layers to reproduce clods and lifts. Specimens were then cured at $20 \pm 2°C$ and $50 \pm 5\%$ in a curing chamber for low drying, to avoid crack formation.

For thermal properties measurement, specimens were oven-dried at 50°C, then wrapped into a plastic film and finally stored at 20°C outside the oven in order to reach temperature equilibrium inside the specimen with the ambience, prior to testing. For water vapour permeability and Moisture Buffering Value (MBV) measurements, specimens were kept at 20°C-50% before the tests.

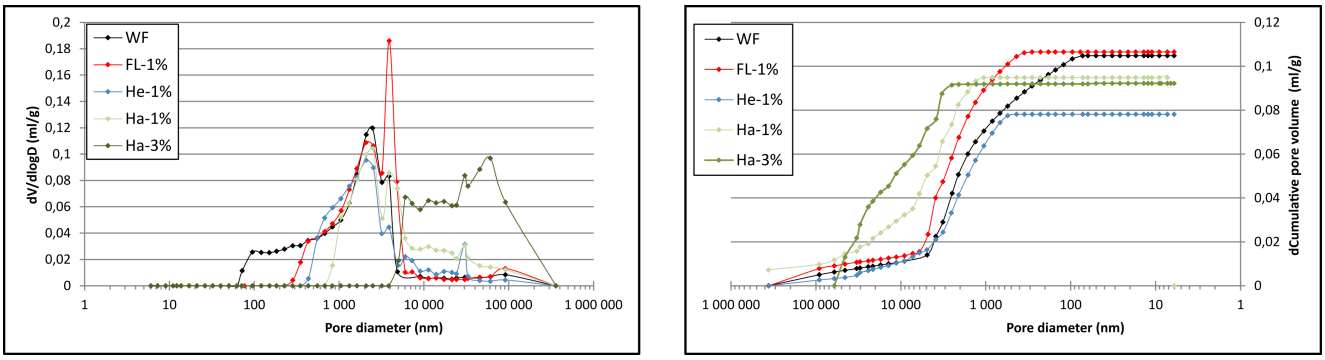

Figure 3: differential porosity distribution curves of mixtures (left) and cumulative distribution curves (right)

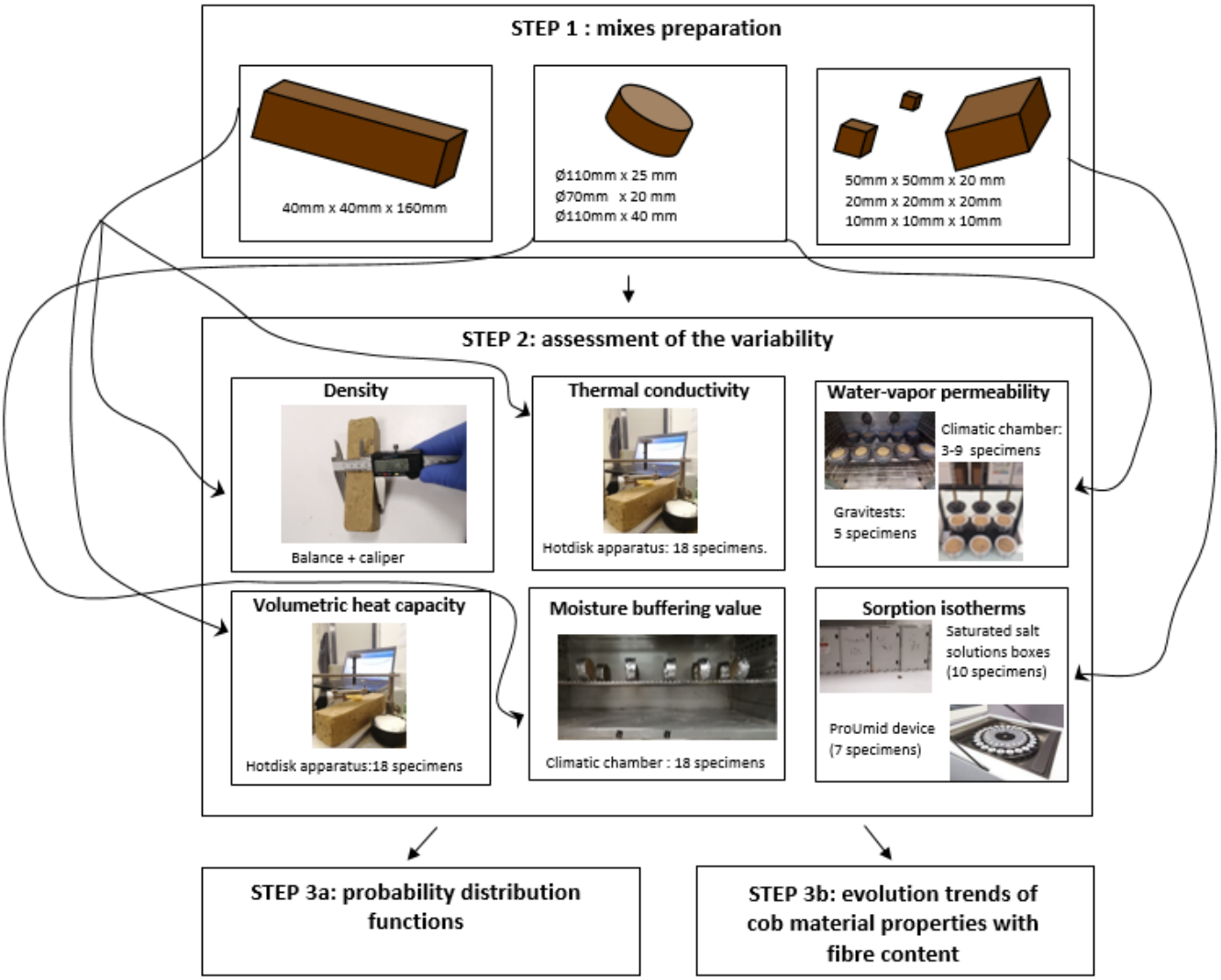

Figure 4: from material formulation until variability assessment

2.2.2. Dry bulk density

The prismatic specimens (160x40x40 mm^3) were oven-dried at 50°C until a constant mass. The specimen mass was measured by means of a laboratory balance providing a 0.01g accuracy and the different lengths of the prism were measured by means of a caliper with 0.01 mm accuracy. The volume drying shrinkage was found to be :

- $13.07 \pm 0.12\%$ for unfibred materials;
- $17.13 \pm 0.96\%$ and 16.44 ± 0.18 for 1% and 3% flax yarns composites respectively;

Table 2: Mixes composition for 100 kg of dry soil

Formula	Description	Dry soil mass (kg)	fibre content		Water content (%)
			mass (kg/100 kg of dry soil)	Particle Volume (m^3/m^3 of dry soil (%))	
WF	Without fibre	100	0	0	19
FL-1%	Flax yarn	100	1	1.81	23
Ha-1%	Hay stalk	100	1	2.40	24
He-1%	Hemp shive	100	1	2.07	25
FL-3%	Flax yarn	100	3	5.44	24
Ha-3%	Hay stalk	100	3	7.21	23
He-3%	Hemp shiv	100	3	6.21	23

- 16.89 $\pm$ 2.41% and 11.57 $\pm$ 0.12 for 1% and 3% hemp shives composites;
- 13.69 $\pm$ 2.02% and 5.13 $\pm$ 0.45 for 1% and 3% hay stalks composites.

The plants fibre increased the shrinkage with regard to unfibred material and increasing the fibre content led to a decrease in the shrinkage as shown in [56,57]. This effect was enhanced for hay stalks composites, highlighting the dimensional stability provided by the latter.

2.2.3. Thermal properties: the Hot disk device

A Hot Disk device was used to measure the thermal conductivity λ and the specific heat capacity ρC_p of specimens from the evolution of the temperature at the interface between the specimen surface and the sensor (thermogram). It is a Transient Plane Source (TPS) measurement technique and the system is made up of: - a Hot Disk sensor made up of nickel alloy 10 μm thick and protected by a Kapton polymer film of 30 μm thick, - a power supply, - a data acquisition system and a post-treatment software.

The measurements were performed assuming that the specimen is (i) a semi-infinite medium (one-sided measurement), (ii) homogeneous and (iii) isotropic. The first assumption was checked by comparing the probing depth and the distance from the hot disk to the nearest boundary of the specimen, that must be greater than the probing depth. Following Gustavson et al mathematical developments [58], the thermal properties can be inferred from the thermogram. A constant heating power of 20 mW is applied by the HotDisk sensor during 20 seconds. The temperature increase is recorded by converting the sensor resistance into temperature (resistive temperature probe).

As the HotDisk gives the values of local properties, the experimental procedure was repeated on the four flat faces of each specimen to obtain a representative value of the thermal conductivity (λ) and of the volumetric heat capacity(ρC_p). The four data were post-processed to find the representative value of each specimen. They were assumed to follow a Student's distribution of $k = 3$ degrees of freedom. The confidence interval of the mean values depends on the chosen significance level $1 - \alpha$ and is given by $\left[\bar{x} - t^3_{\alpha/2}.\frac{\sigma}{\sqrt{4}} \quad \bar{x} + t^3_{\alpha/2}.\frac{\sigma}{\sqrt{4}}\right]$; where $\bar{x}$ is the mean of the four measured data; $t^3_{\alpha/2}$ is the third order quantile of student's law at the significance level of $1 - \alpha/2$, computed by finding the probability that the random variable X that hold the four data is $1 - \alpha$; σ is the standard deviation. λ and $\rho.C_p$ for each specimen are calculated as the average value of the data inside the computed interval. This can lead to discard one of the four values or none of them. A significance level $\alpha = 90\%$ was chosen as still 75% the total coefficient of variation of mixtures were quite steady.

As example, Figure 5a shows the scatterings of λ measurement performed on the 18 specimens for He-3% mix. It seems that the representative value property of a specimen is not always the mean value of the four data. Indeed, thermal properties at the some interface were more or less discarded from the 03 others measurements. Thereafter, square-surrounded values were omitted for the computation of specimens representative mean and CV of mixes properties.

In order to discard the negative effect of the air gap thermal resistance between the specimen and the probe and of the time gap between two measurements carried out on the same specimen [59, 60], repeatability tests

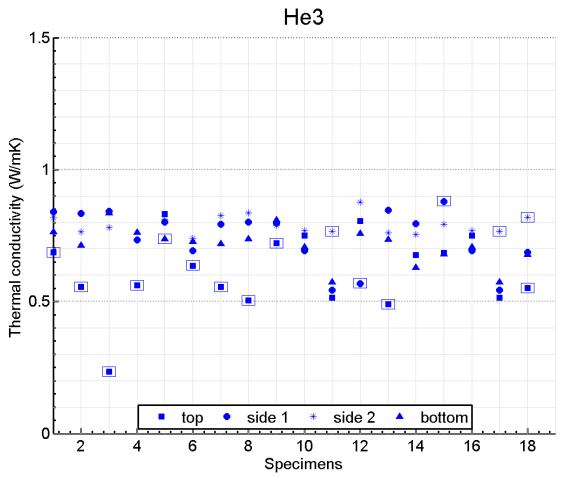

(a) Thermal conductivity: He-3% mix

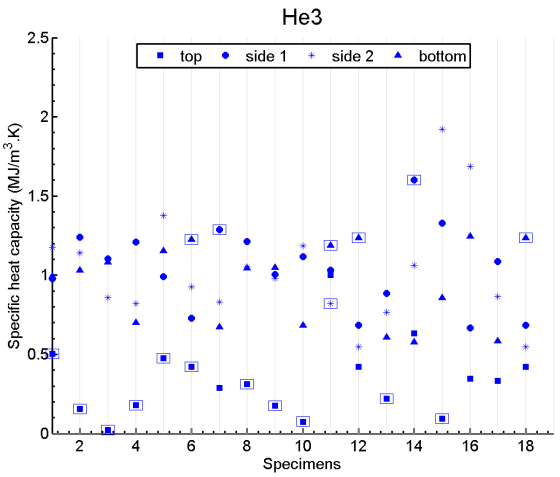

(b) Specific heat capacity: He-3% mix

Figure 5: Variability of λ and $\rho.C_p$ for each specimen of He-3% mix. Squared-surrounded data were omitted to find the mean representative value of each specimen and to compute CV of mixtures.

were performed on twenty specimens. The related variance V_{Press} and V_{rad} were then evaluated. Using a variance decomposition model, the intrinsic variance V_{int} (equation 1) and the related coefficient of variation CV_{int} (equation 2) were determined. After calculation, negligible effects were found on the total coefficient of variation for λ.

$$V_{int}(k) = V_{tot}(k) - max(V_{press}(k); V_{rad}(k)) \quad \text{(equation 1)}$$

$$CV_{int}(k) = \frac{\sqrt{V_{int}(k)}}{\mu(k)} \quad \text{(equation 2)}$$

where :

- $V_{int}(k)$: Intrinsic variance of property k
- $CV_{int}(k)$: Intrinsic coefficient of variation of property k
- $\mu(k)$: mean value of the property k

2.2.4. Water vapour permeability

The water vapour permeability was determined by means of the dry cup test (DCT) technique (gravimetric method - NF EN ISO 12572:2016 Standard [61]), both manually (manual DCT) and automatically (Gravitest device [62]).

Both consist in filling a cup with silica gel imposing a relative humidity of 3% inside the cup and closing the cup with the studied material. The cup was sealed with silicone to ensure air tightness. The cup was then placed into a room at 23°C and 50% relative humidity. A water vapour flux appears consequently from the ambient air into the cup because of the vapour pressure gradient, yielding an increase in the cup mass. The evolution of the cup mass was measured until constant water vapour flux through the specimen (relative error lower than 5% of the five last tests mean). The specimens dimensions were $\phi 110 \times 25mm$ using the manual DCT and $\phi 70 \times 25mm$ for the Gravitest device.

To assess the water vapour permeability, the fluxes were corrected by taking into account the air gap between the surface of silica gel and the material ($d_a = 3cm$).Tests were performed on 3-8 specimens per mix.

Repeatability tests were performed on 3 mixes specimens (WF, Ha-1% and FL-1%) by re-sealing specimens and changing the silica gel (and change the width of the air-gap between the silica gel and the specimen surface). Relative errors of 1%, 3% and 13% respectively were found for WF, Ha-1% and FL-1% respectively.

2.2.5. Sorption isotherms

Sorption isotherms were measured by the means of the ProUmid device (7 specimens) [62] and the Saturated Salt Solutions (SSS) method (10 specimens) at 23°C.

The SSS method consists in saturating salts in sealed boxes, able to impose the relative humidity (RH) of the inner environment at various RH levels : 12%, 33%, 55%, 65%, 76%, 86% and 97%. $50 \times 50 \times 20mm^3$ specimens were used. The equilibrium moisture content was set for a relative mass variation of specimens lower than 0.5%.

The principle of the ProUmid device is the same as for SSS method, but the weighing and RH level change operations are automatic. The relative error of mass variation was set at 0.01%. The specimens were dried at 50°C and placed into the apparatus. The specimens follow firstly vacuuming operation to achieve a full drying process prior to the change in the RH level. The water content of the specimens were measured at 0% - 10% - 20% - 30% - 40% - 50% - 60% - 70% - 80% - 90% - 95% RH, on $10 \times 10 \times 10mm^3$ cubic specimens. Two cases of tests were considered for SSS:

- case 1 : specimens were dried and then, were submitted to an adsorption/desorption cycles (5 specimens for SSS method and 7 for ProUmid).
- case 2: specimens were saturated by a weak stream of water and then were submitted to a desorption/adsorption cycle (5 specimens for SSS method).

The drying process was done in an oven at $50°C$ for SSS. ProUmid proceeds to a vacuuming operation of specimens. The humidification process (weak stream of water particles) is an adjustment for earthen material of the NF EN ISO 12571:2021 standard [63], that advises to saturate the specimens (and eventually following a depressurizing operation to speed up the desorption process).

At the end of the tests, the specimens of the SSS were microwave-oven dried to remove the residual water. The water content inside the material was then computed for different relative humidities.

2.2.6. Moisture Buffering Value (MBV)

The tests were performed according to the NORDTEST protocol [64]. The lateral surface of the specimens was sealed by a paraffin layer and then an aluminium tape and cured at 23°C and 50% relative humidity until equilibrium. Thereafter, specimens were disposed into a climatic chamber at 23°C and submitted to a daily relative humidity loading cycle of 75% RH during 8 hours and 33% RH during 16 hours. Specimens were then weighed regularly every 2 hours during the adsorption cycle and twice during the desorption one.

The daily protocol was repeated until the difference in mass variation of the specimens was lower than 5%. The Moisture Buffering Value MBV was then calculated as the ratio of the mean mass variation of the two last cycles by the exchange surface of the specimen (A) and the gap of RH between cycles. The NORDTEST protocol provides the material classification with respect to the moisture exchange capacity by the MBV (see table 3). The tests were performed on 18 specimens.

Table 3: Material humidity exchange quality according to its MBV value [64]

MBV Value	0 - 0.17	0.17 - 0.50	0.50 - 1.00	1.00 - 2.00	2.00 - 4.00
Material performance	negligible	limited	Moderate	good	Excellent

2.3. Probability Density Function (PDF)

For the different properties of the studied materials, the experimental data were used to compute the probability density functions (PDFs) and derive the parameters of three Distribution Models (DMs): **the Normal law, the Lognormal law, the Weibull law**. The mathematical models are described in table 4.

To determine the experimental PDFs, the range of variation of a parameter was divided into a number of sub-intervals depending on the number of experimental values. Each sub-interval corresponds to a bin on the graphical representation of the experimental PDF. To do so, empirical Sturge and Fredman-Diaconis rules were used to find

Table 4: Distributions models: E(.) represents the expectation, Std(.) is the standard deviation and $\Gamma(.)$ is the Euler-Gamma function

DM	pdf(x)	parameters	Expectation (m)	Variance (s^2)
Normal	$\frac{1}{\sigma\sqrt{2\pi}} exp\left[-\frac{(x-\mu)^2}{2\sigma^2}\right]$	μ = E(x) σ = Std(x)	μ	σ^2
Lognormal	$\frac{1}{x\sigma\sqrt{2\pi}} exp\left[-\frac{(ln(x)-\mu)^2}{2\sigma^2}\right]$	μ = E(ln(x)) σ = Std(ln(x))	$e^{\mu+\sigma^2/2}$	$(e^{\sigma^2}-1)e^{2\mu+\sigma}$
Weibull	$\frac{k}{\lambda}\left(\frac{x}{\lambda}\right)^{k-1} exp\left[-\left(\frac{x}{\lambda}\right)^k\right]$	λ: scale k: shape	$\lambda\Gamma\left(1+\frac{1}{k}\right)$	$\lambda^2\Gamma\left(1+\frac{2}{k}\right)-\mu^2$

the number of bins. The former led to a fixed number of bins for almost all properties (**5 bins**) while the latter led to a variable number of bins from one property to another according to the interquartile range of data (**4-6 bins**).

A sensitivity analysis was performed according to the number of Bins Clustering (BC) of experimental data (4-6) to find the best fit. The number of bins was chosen using the statistical significance of fits through p-values, obtained after a χ^2 goodness-of-fit test. It represents the probability that the null hypothesis (the experimental distribution fits the DM), have chances to be satisfied. The threshold proposed on this paper was 5%. The DM statistical parameters were then computed: mean, standard deviation and CV (CVm), according to the relations between the expectation and the variance and the parameters of each model given in table 4. The CV values derived from the least-square adaptation of the different models on the experimental data were compared to the experimental CV values (CVe).

3. Results and discussions

3.1. Variability of the properties

3.1.1. Variability of the dry bulk density (ρ)

Figure 6 shows box-plots of the dry bulk density and the mean values for each formulation (black squared dots). The mean value of each mix shows that the addition of plant fibres yields a decrease in the material density, as previously shown by Laborel et al [6].

The results show that the dry bulk density is influenced by the fibre content, that generally induces a decrease in the dry bulk density, except for flax for which a slight increase is observed between WF and FL-1%. Nevertheless, for increasing values of the fibre content, all the fibred materials show a decrease in ρ. In fact, the soil is at least twice as dense as plant fibres. However, this latter does not take into account the change in the porosity induced by the addition of fibres, as shown by both the optical microscopy and the mercury porosimetry data.

The unfibred material exhibits the highest variability in the dry bulk density as this parameter ranges from 1754 to 1952 kg/m^3 ($\Delta\rho = \rho_{max} - \rho_{min} = 198kg/m^3$). This highest variability is confirmed by the values of the statistical indicators CV=2.96% and IR = $63kg/m^3$ (tables 6 and 7). Compared to the reference WF mix, a drop in the variability can be observed for 1% fibred composites, both for CV and IR:

- for FL-1% : 68% for CV and 61% for IR;
- for Ha-1% : 60% for CV and 59% for IR;
- for He-1% : 28% for CV and 30% for IR.

FL-1% mix has a mean value slightly greater than WF mix (1845 and 1837 kg/m^3 respectively) and showed the lowest variability with an IR of 24 kg/m^3. It was the less variable among mixes for the density. Next come Ha-1% composites, with a CV of 1.17% and then He-1% with a CV of 2.13%.

Flax yarns composites show at 1% and 3% fibre contents (FC) densities of 1845 kg/m^3 and 1742 kg/m^3 which are 5% to 17% higher than the 2 others composites. That is explained by the thin diameter of the fibres, that easily spread into the earth matrix and yield a decrease in the material porosity. Composites exhibit a low decreasing

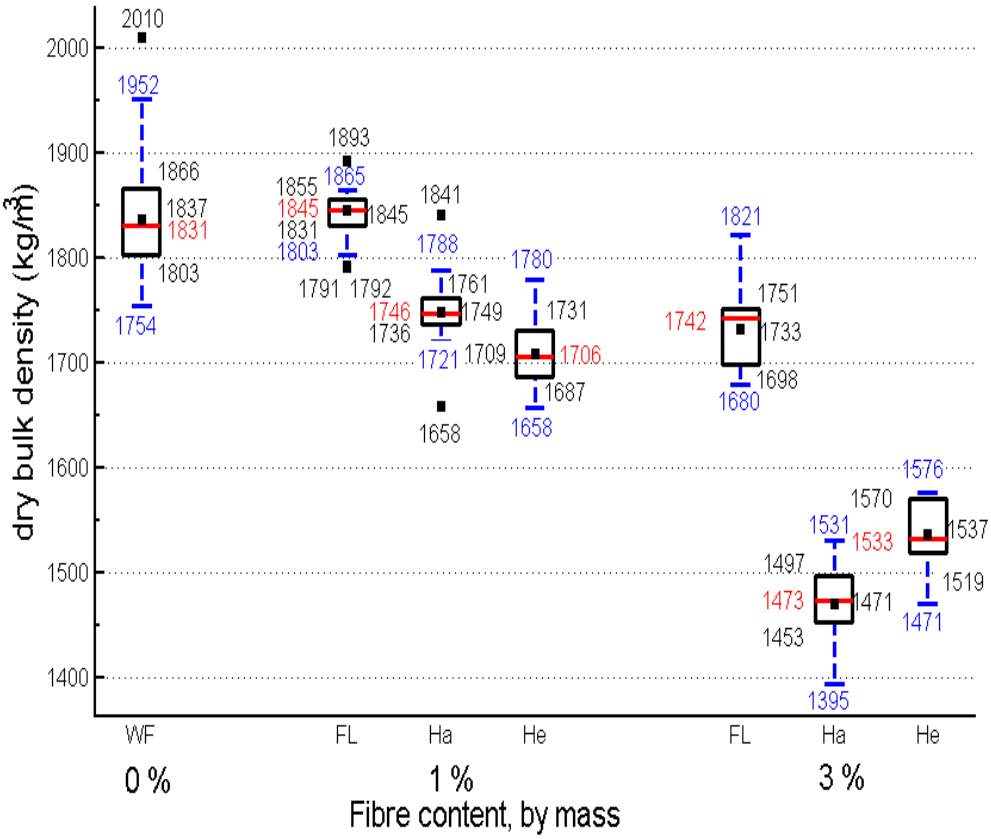

Figure 6: Variability of the dry bulk density of cob materials with respect to plant specie and the fibre content.

rate $\tau = \dfrac{\rho_{3\%} - \rho_{1\%}}{\rho_{1\%}\,(3\% - 1\%)}$ in the values of the density from 1% to 3% FC of **3% with Flax, 8% with Hay and 5% with Hemp.**

Increasing the FC increases the variability of the measured density values. The same trend is found by [20,54]. The deduced values of CV increase from 0.94% to 2.09% for FL; from 1.17% to 2.50% for Ha. For He mix, the CV were close to each other (2.13% and 1.83%). Using IR confirms the increase in the variability (from 44 to 51 kg/m^3). According to Niyigena et al [20], a variability can be considered "negligible" when the CV falls under 10% - but a sensitivity analysis on the energy performance assessment is necessary to confirm this assumption.

3.1.2. Variability of the thermal conductivity (λ)

Figure 7 describes the variability using box-plots for the thermal conductivity of mixes, regrouped according to the fibre content. Like for densities, flax-fibred composites exhibit the highest average thermal conductivity. WF mix show a variation range of 0.99-1.15 W/(m.K) close to FL-1% material. Ha-1% and He-1% vary between 0.80 and 1.00 W/(m.K). FL-3% composites show a variation range of 0.90-0.98 W/(m.K), Ha-3% from 0.58 to 0.83 W/(m.K) and He-3% from 0.68 to 0.82 W/(m.K). Tables 6 and 7 display the total and the intrinsic CV and the interquartile Range (IR), respectively. The IR was used as the variability indicator, as it does not take into account the outliers. For a fibre content of 1%, the highest variability if obtained for Ha-1% with an IR of 0.073 W/(m.K). Next comes He-1% with an IR of 0.061 W/(m.K).

For increasing FC, the highest variability is found for He-3% with an IR of 0.079 W/(m.K) while Ha-3% IR is equal to 0.065 W/(m.K). Moreover, a decreasing variability per FC of 28% was observed for Flax composites, 11% for hay composites and a increase in the variability of 30% for hemp composites (using IR). The high variability of hemp composites is also linked to the length variation of hemp shives (0.6-17 mm [48]). This is in accordance with previous research works performed by Laibi et al [29], Ba et al [65] and Millogo et al [66], that have shown a decreasing effect on the thermal conductivity with the fibre length in earthen composites with Kénaf, Typha and

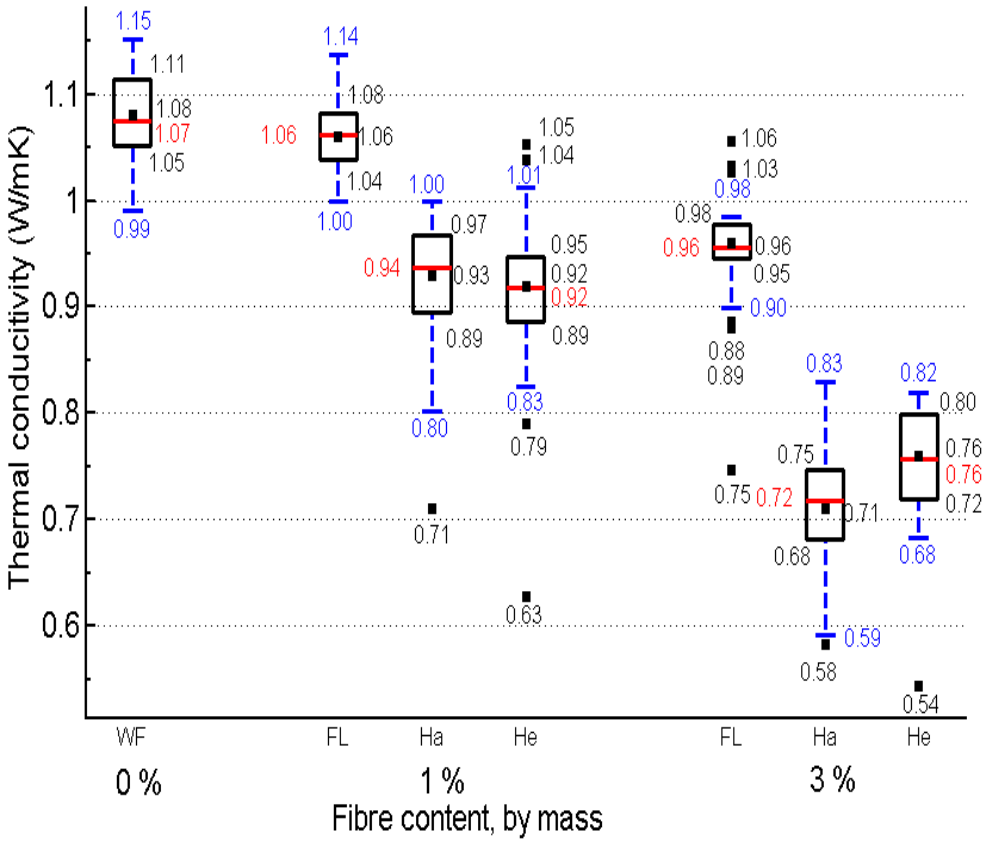

Figure 7: Variability of the thermal conductivity of cob mixtures according to the fibre specie and content.

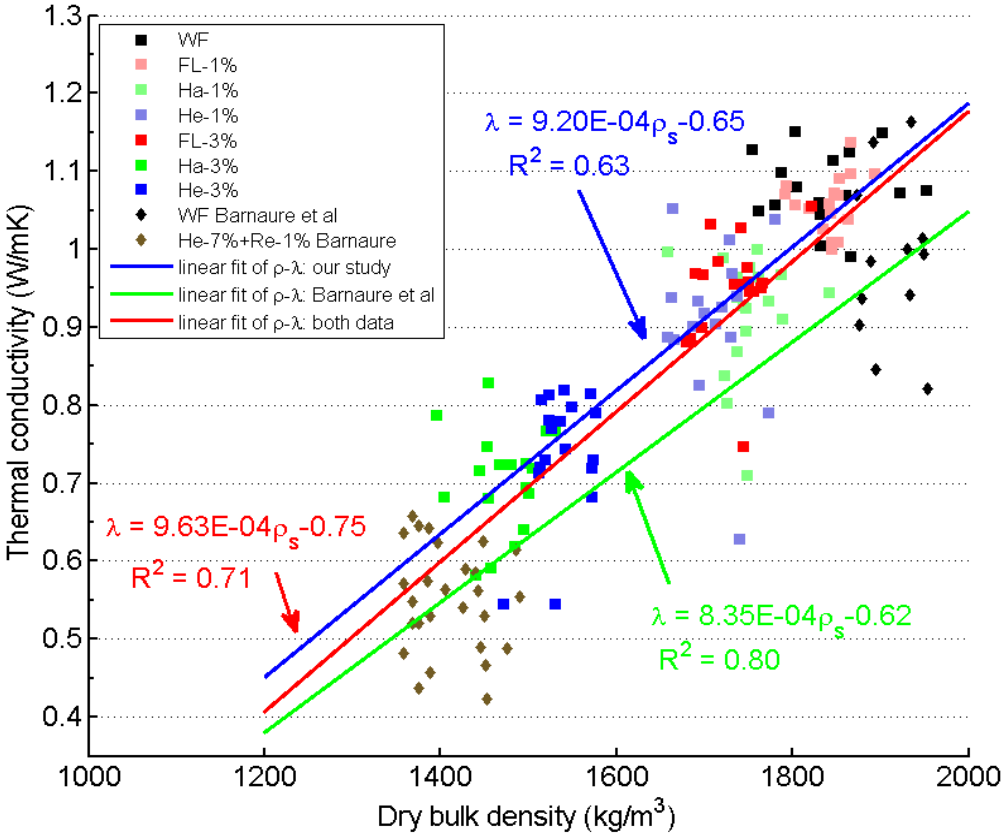

Figure 8: correlation between the density and the thermal conductivity

Hibiscus cannabinus fibres, respectively.

Compared to unfibred materials, a decreasing variability of $\frac{\lambda_{WF}-\lambda_{FL-1\%}}{\lambda_{WF}} = 31\%$ for FL-1% and 2% for He-1% (using IR). While, it was found an increasing variability of 18% for Ha-1%. A decreasing variability with FC of $\frac{\lambda_{FL-3\%}-\lambda_{FL-1\%}}{\lambda_{FL-1\%}} = 28\%$ was found for Flax composite, 11% for Hay composites was found and a variability increase of 23% for Hemp composites. A close discussion will be done in section 4.2.

Figure 8 shows the correlation between the dry bulk density and the thermal conductivity using the mean values (outliers were removed). A negative correlation between the thermal conductivity and the FC was found like in [66, 67]. A linear model was applied to the experimental data to obtain the relationship between λ and ρ : $\lambda = 9.14E-4 \times \rho_s - 0.65$. For this density range, a similar relationship was found by Barnaure et al [54] ($\lambda = 8.35E-4 \times \rho_s - 0.62$). These data were obtained with the same earth but with different plant fibres (hemp shiv and reed). This is a commonly observed evolution of the thermal conductivity with the density.

3.1.3. Variability of the specific heat capacity ($\rho.C_p$)

Figure 9 displays the variability of the specific heat capacity of composites, regrouped according to the fibre content. The variability of ρC_p is very different for the different formulations and it can not be explained neither by differences in the homogeneity of the material, nor by differences in the porosity. One explanation is that the HotDisk technique is not always reliable for the measurement of ρC_p.

By comparing the mean values, we found quite the same value of $\rho.C_p$ for Ha composite (0.950 and 0.980 MJ/MJ/(m^3.K)), a negative correlation for FL and He composites. In comparison to WF mix, FL-1% and FL-3% exhibit a low variability (IR of 0.119 MJ/MJ/(m^3.K) and 0.111 MJ/MJ/(m^3.K) respectively vs 0.195 MJ/MJ/(m^3.K) for WF mix). Flax composites show a quite stable variability rate from 1% to 3% FC unlike hay composites, which showed a decreasing variability by a rate of 2 MJ/MJ/(m^3.K) per FC (IR of 0.428 MJ/MJ/(m^3.K) and 0.140 MJ/MJ/(m^3.K) respectively). As same values, Hemp composites showed a decreasing variability range (IR of 0.503 MJ/MJ/(m^3.K) at 1% FC and 0.218 MJ/MJ/(m^3.K) at 3% FC). Hay and Hemp composites exhibited the highest variability. That could be correlated to the size of fibre variation for hemp composites, and to the mix of plant bark and leaves for Hay stalk composites. This increases heterogeneity of hay composites. This is also explained by MIP tests, where these mixes show a variability of these micro-structure textures (figure 3). Indeed, Ha-3% mix has shown a quite uniform distribution from 40 μm to 400 μm pore diameter. In the same way, Ha-1% have shown a large scale of pore diameter, in contrast to other formulations.

3.1.4. Variability of the water vapour permeability k_m

Figure 10 shows the variability of the water vapour permeability for the two measurement methods (manual DCT and Gravitest). Box-plots were not performed because of the low number of specimens. Both the manual DCT and the Gravitest were performed on WF and the fibred formulations with FC of 1%. For the fibred formulation with FC of 3%, only the manual DCT was carried out.

The mean value of k_m for WF is almost the same whatever the measurement method (means of $9.13 \times 10^{-12} kg/(m.s.Pa)$ using manual DCT and $8.26 \times 10^{-12} kg/(m.s.Pa)$ using the Gravitest). While for other mixes, difference can be observed on the mean values, although they are of the same order of magnitude for a given formulation. The values determined from manual DCT are however greater than the values given by the Gravitest. The Gravitest results show also a lower variability than the manual DCT, even if the number of tested specimens is too low to get a general conclusion about the better performance of the Gravitest.

We found a slight decrease of k_m with hemp shives and hay stalk content (from $1.14 \times 10^{-11} kg/(m.s.Pa)$ to $8.94 \times 10^{-12} kg/(m.s.Pa)$ for He composite, from $1.32 \times 10^{-11} kg/(m.s.Pa)$ to $1.05 \times 10^{-11} kg/(m.s.Pa)$ for Ha composite). While, k_m of Flax yarns increased (from $8.16 \times 10^{-12} kg/(m.s.Pa)$ to $6.48 \times 10^{-11} kg/(m.s.Pa)$).

Table 5 shows the coefficient of variation of k_m for the different formulations according to the measuring method. The last two columns of the table combine the results of both techniques. Contrary to the thermal properties, the variability ranges were higher, certainly due to the low number of specimens. For WF specimens, the CV for Gravitest was 12% higher than manual DCT with a global CV of 11%.

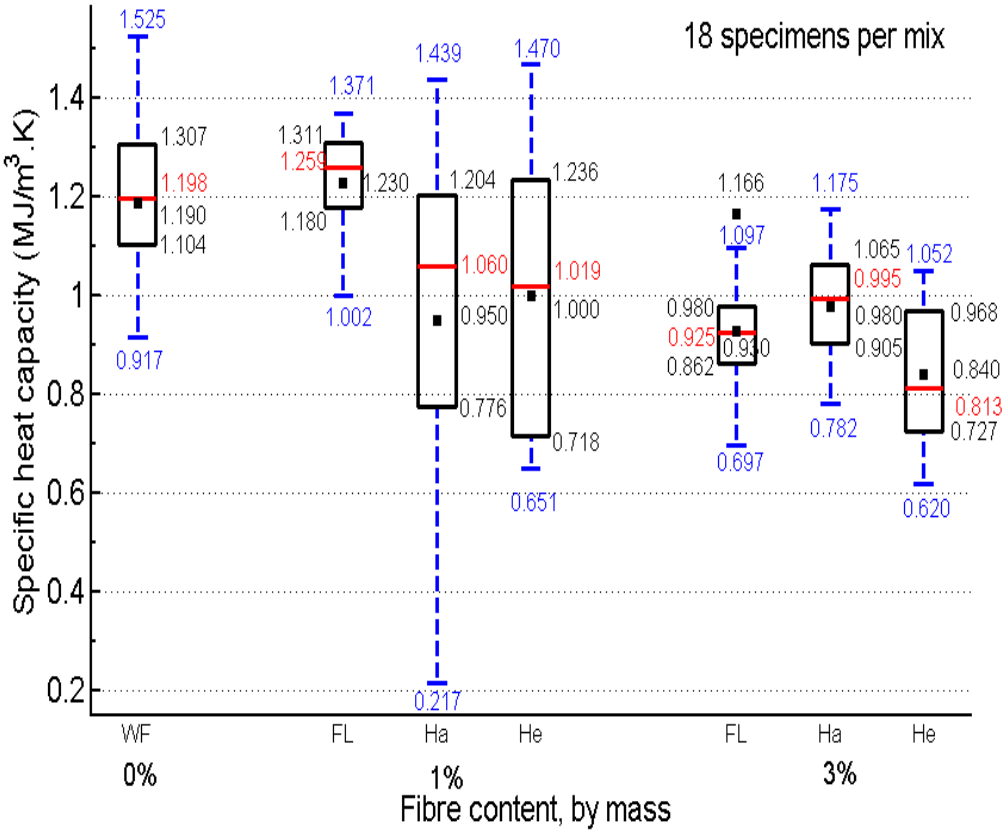

Figure 9: Variability of the specific heat capacity of cob materials with the plant add-ons used and the fibre content.

For He-1% and FL-1% composites, CVs of 50% and 56% were found using manual DCT while, 7% and 14% were found using Gravitest.

Lower values were found for He-3% and FL-3% (19% and 27% respectively using manual DCT). For Hay stalk composites, there is a low increase in CV with manual DCT by 11%.

3.1.5. Variability of the sorption isotherms

Figure 11 shows the variability of sorption isotherms using SSS boxes and the ProUmid device, for the two cases (see section 2.2.5). It has to be noticed that the curves are represented by straight lines between two dots and that for the desorption curves, the value at 13% RH is not present, which can yield the misleading conclusion that the water content is higher during the adsorption phase than during the desorption phase. This is actually not the case.

The water content values of the adsorption and desorption curves measured by SSS were higher than those obtained with the ProUmid device for most values of the imposed RH. Indeed, at higher RH loads (84%-97%), both methods show quite the same water contents but with greater variability for the SSS method. Even if the results obtained with the ProUmid device look repeatable, it must be remembered that the specimen volume is only 1000 mm^3, which can state the issue of the representativeness of the specimens regarding the moisture sorption, especially for those containing large fibres.

Among the 1% fibre composites, He-1% showed the highest water content for all the RH loads and WF mixture showed the lowest. At 97% RH for He-3% mixture, the mean values of 56 g/kg and 53 g/kg were achieved using SSS and ProUmid (at 94% load respectively for the latter). Increasing the Hay content showed a decrease in the water content, but this latter is related to the material density too.

Case 2 shows higher water contents with a mean difference of 8.2 g/kg for WF mix, 8.4 g/kg for He-1%, 9.0 g/kg for FL-1% and 6.4 g/kg for Ha-1% for 97% RH loads. This means that there exists a non-negligible

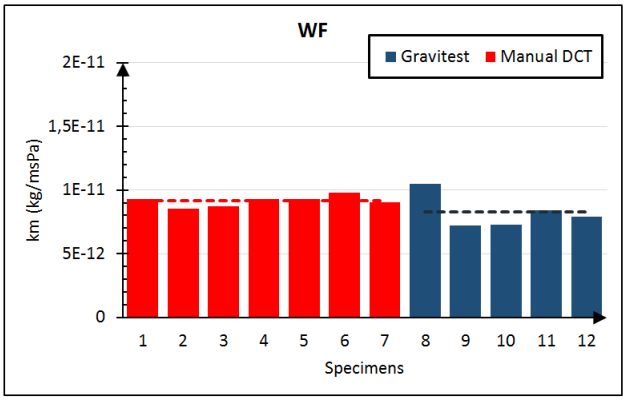

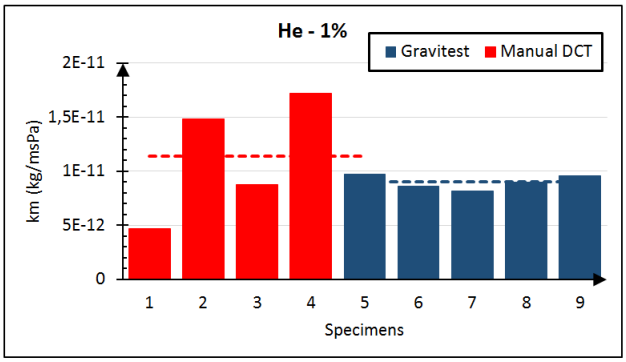

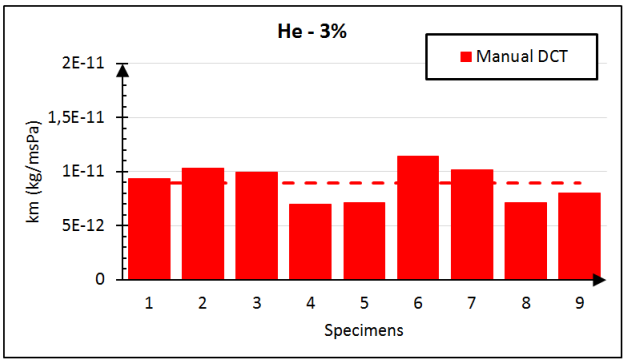

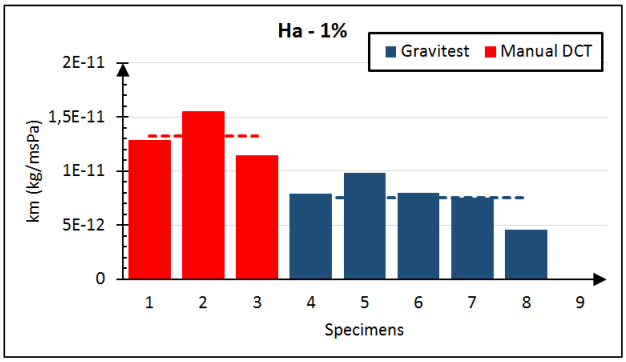

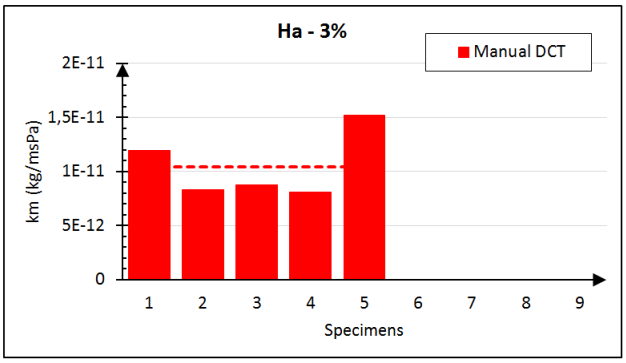

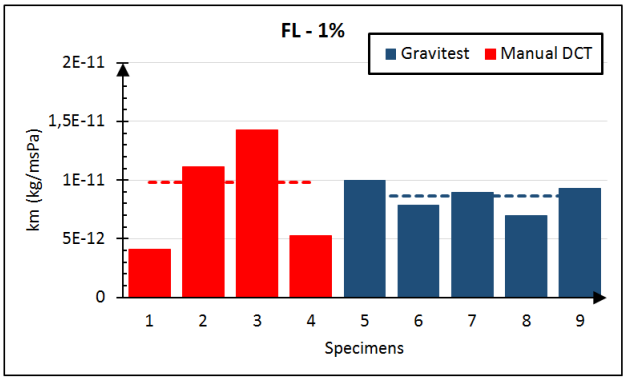

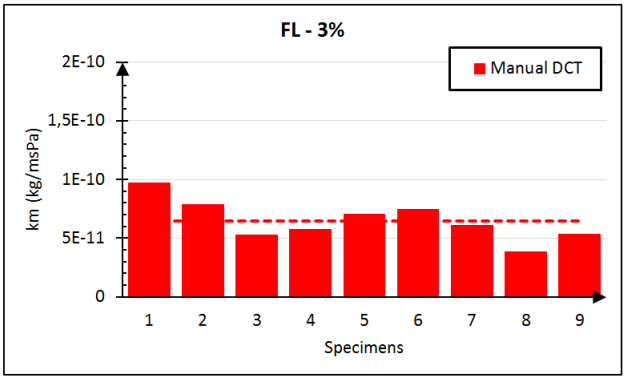

Figure 10: Variability of water vapour permeability according to the mix and the measurement method.

Table 5: Mean and CV of water-vapor permeability according to the mix and the batch

	Manual DCT		Gravitest		Total	
	mean (kg/m.s.Pa)	CV(%)	mean (kg/m.s.Pa)	CV(%)	mean (kg/m.s.Pa)	CV(%)
WF	$9.13x10^{-12}$	4.49	$8.26x10^{-12}$	16.30	$8.46x10^{-12}$	11.71
He-1%	$1.14x10^{-11}$	50.05	$9.01x10^{-12}$	7.25	$1.01x10^{-11}$	37.09
FL-1%	$8.69x10^{-12}$	55.73	$8.26x10^{-12}$	13.92	$8.65x10^{-12}$	35.66
Ha-1%	$1.32x10^{-11}$	15.84	$7.51x10^{-12}$	25.09	$9.66x10^{-12}$	36.02
He-3%	$8.94x10^{-12}$	18.49	-	-	$8.49x10^{-12}$	18.49
FL-3%	$6.48x10^{-11}$	26.71	-	-	$6.48x10^{-11}$	26.71
Ha-3%	$1.05x10^{-11}$	26.90	-	-	$1.05x10^{-11}$	26.90

hysteresis at 97% RH load. The desorption hygric capacity for the case 2 was higher than for the case 1 (e.g: 4.9 kg/kg.%RH vs 1.6 kg/kg.%RH between 65% RH and 86% RH for He-3%).

Figure 12 shows the evolution of CV using ProUmid device for all mixes. WF material shows a similar CV whatever the RH load (around 7%) during adsorption and desorption.

Mean CV values were found from 28% to 94% RH loads of 4.3% for He-1%, 4.5% for FL-1%, 3.4% for Ha-1% and 5.8% for Ha-3% for the adsorption isotherms. The fibred composites with FC=1% showed almost the same CV whatever the fiber type while WF showed greater water content variations. Increasing hay FC increases also the variability of Hay mixes sorption ability.

Figure 13 shows the variability (CV) of the water content for 5 formulations using SSS method and for the two cases. A difference of CV can be seen between 12% RH load (higher CVs) and the others. From 33% of RH load to 97%, a steady decrease in the value of CV was noticed for each mix (CV lower than 5% for 1% fibred composites). Greater variabilities can also be observed during the adsorption phase for Ha-3%, whatever the case, than during the desorption phase. During this latter, the values of CV were not greater than 12%, wherease they were as high as 23% during the adsorption phase.

FL-1% showed lower variations for case 2 than for case 1 in adsorption and desorption when RH load is higher than 33%, confirming the homogeneity of that composite. This is estimated between 2% and 3%, according to RH level. Increasing hay stalk content increased the variability of the water content of materials by a factor of 2 by mean (for the case 1). They are emphasized at 12% and 97% RH load (18% and 12% more respectively). Same observations for WF specimens: that is directly correlated to the microstructure as shown on porosity distribution curves where there are a large range of pore sizes for WF and Ha-3% specimens (section 2.1).

A high variation of the hysteresis was noticed at low humidity levels with the ProUmid device (9.5% - 19%) for every mixes (figure 14). Starting from 28% RH load until 85.5%, there was lower CV of hysteresis ranging from 3% to 10%.

3.1.6. Variability of the moisture buffering value (MBV)

Figure 15 shows the variability of the MBV values and table 6 the CVs. As can be seen, the addition of plant fibres increases the moisture exchange capacity of cob materials. They were almost all classified as "good", as the values of the MBV range between 0.9 and 1.2 for WF, and between 1.5 and 2.0 for composites. Fibred specimens showed almost the same MBV values by mean and close values of CV. There was not noteworthy increase in the variabilities of MBVs from 1% to 3% FC range. The WF mix showed the highest variability with a CV of 9.78%. CV was 5.73% and 5.66% for FL-1% and FL-3% mixtures, 6.51% and 5.08% for Ha-1% and Ha-3% mixes, 3.52% and 6.99% for He-1% and He-3% mixes.

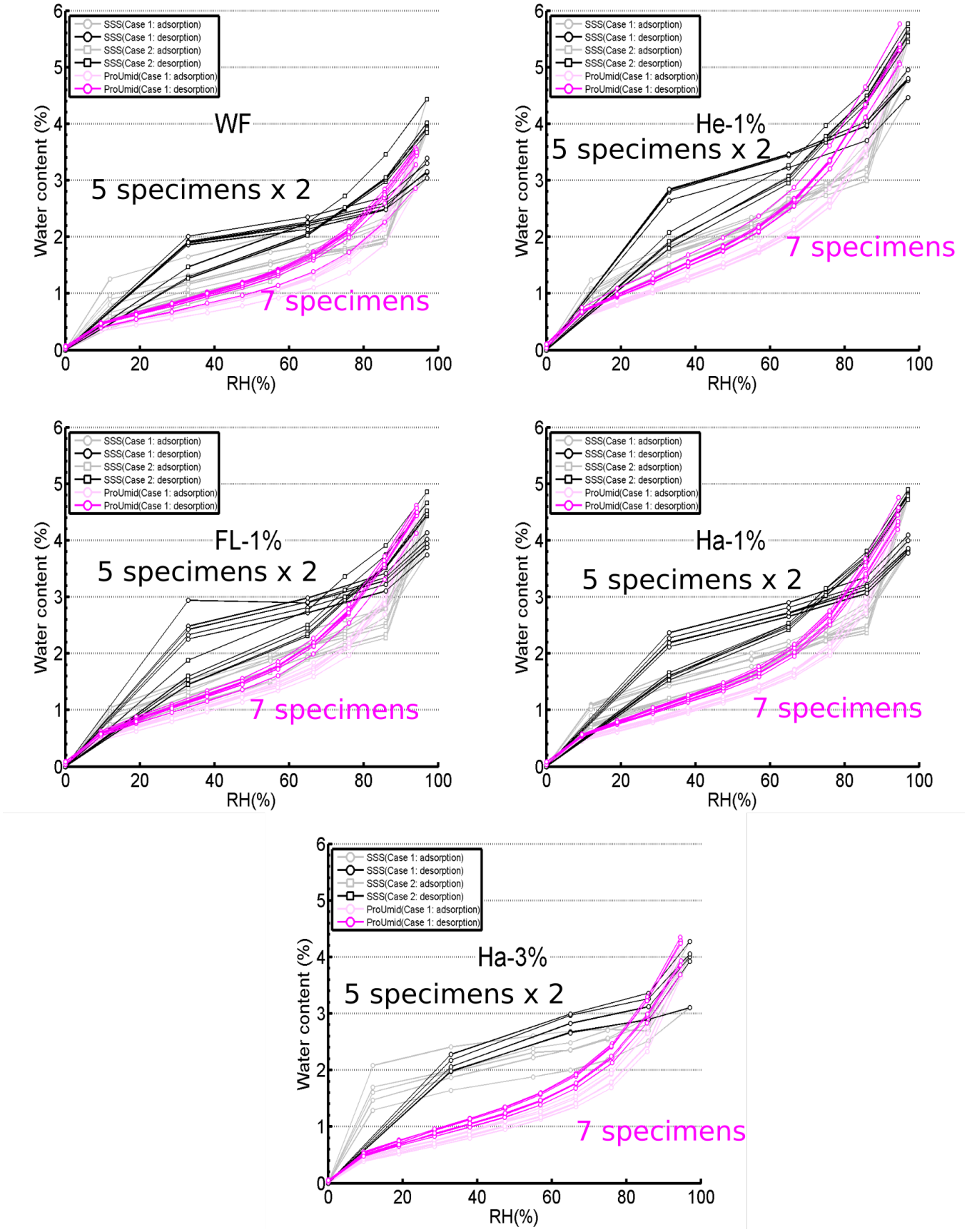

Figure 11: Variability of sorption isotherms for each mix. Case 1 and Case 2 protocols are described in section 2.2.5

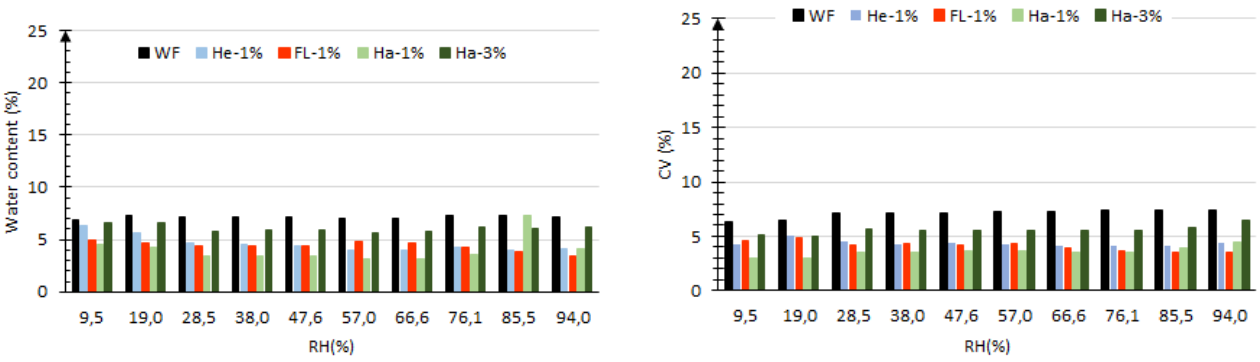

(a) Adsorption

(b) Desorption

Figure 12: Water content CV of sorption isotherms using ProUmid device (case 1)

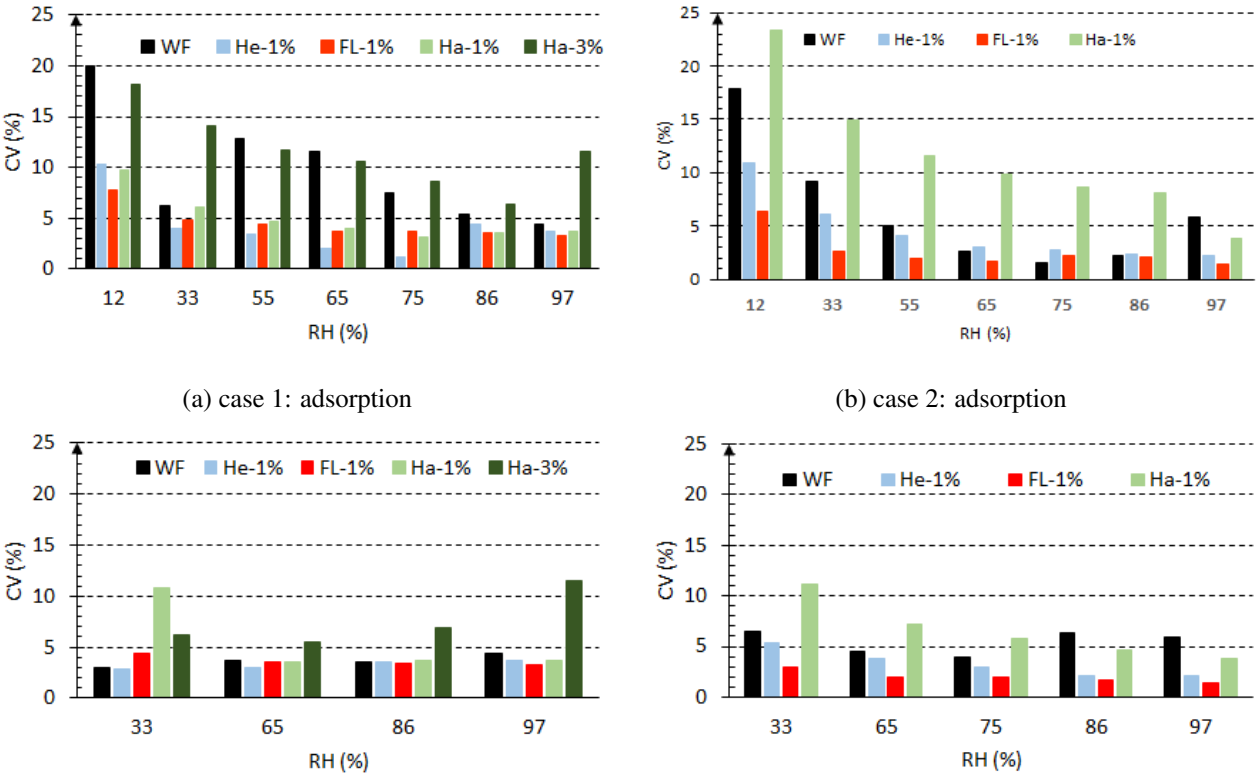

(a) case 1: adsorption

(b) case 2: adsorption

(c) case 1: desorption

(d) case 2: desorption

Figure 13: Water content CV of sorption isotherms using SSS method

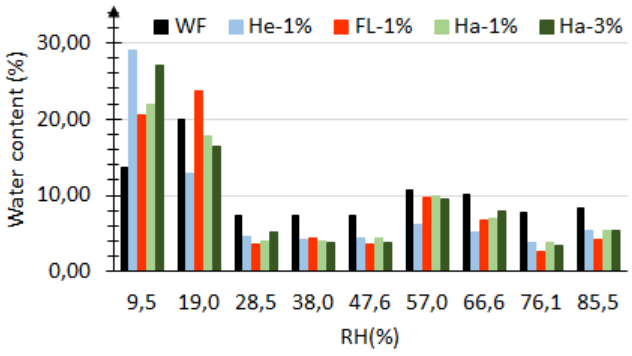

Figure 14: Variation of the hysteresis according to the mix and the RH load, using ProUmid device

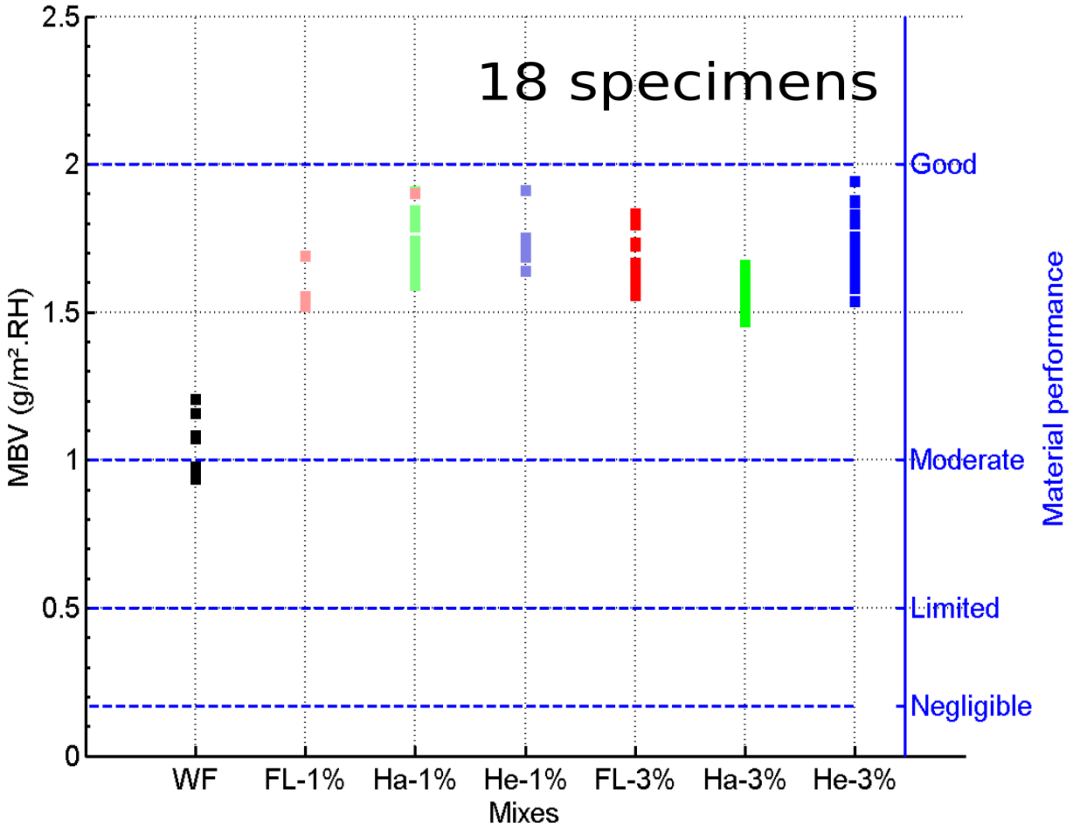

Figure 15: Variability of MBV tests and classification according to the NORDTEST protocol

Table 6: variability of the material properties - coefficient of variation (CV)

	WF	**FL-1%**	**FL-3%**	**Ha-1%**	**Ha-3%**	**He-1%**	**He-3%**
				Total variability			
Dry bulk density	2.96	0.94	2.09	1.17	2.51	2.13	1.83
Thermal conductivity	4.13	3.34	7.19	8.18	9.37	10.89	11.06
Specific heat capacity	12.64	8.31	12.58	36.19	11.35	26.66	14.97
MBV	9.78	5.73	5.66	6.51	5.08	3.52	6.99
				Intrinsic variability			
Thermal conductivity	3.70	2.88	6.99	7.71	8.61	9.57	10.88
Specific heat capacity	11.79	6.91	10.52	35.07	6.58	23.71	14.01

Table 7: variability of the material properties - interquartile range (IR)

	WF	**FL-1%**	**FL-3%**	**Ha-1%**	**Ha-3%**	**He-1%**	**He-3%**
Dry bulk density (kg/m^3)	63	24	53	25	44	44	51
Thermal conductivity (W/mK)	0.062	0.043	0.031	0.073	0.065	0.061	0.079
Specific heat capacity (MJ/m^3.K)	0.195	0.119	0.111	0.428	0.140	0.503	0.218
MBV (g/m².%RH)	0.15	0.09	0.10	0.16	0.08	0.05	0.17

4. Distribution of cob properties and analysis

4.1. Probability density function (PDF) of cob properties

For mixes density, thermal conductivity and specific heat capacity, p-values were always greater than 5% whatever the distribution model (DM) and the bins clustering (BC) of the data. Therefore, the models appear to be reliable to assess the PDF of properties. Figures 16, 17 and 18 display the best PDF (according to the p-value), that is to say the lognormal models for the density, the thermal conductivity, the specific heat capacity, the moisture buffering value and the water content of the sorption isotherms for various RH loads. For this latter, the PDF were calculated for each value of the RH. Tables 8 and 9 display the computed statistical parameters and the comparison between the CV values deduced from the parameters of the models and the experimental CV values.

For mixes densities and thermal properties, we found centered DMs, except for $\rho.C_p$ of Ha-3% mix which shows a low skewness. Across mixes, the spreads follow the same range as computed variability parameters, in particular FL mixtures. FL-1% shows a low spread compared to WF as found IR, as confirmed by the coefficient of variations ranging from 1.46-1.62 vs 3.57-4.85 for WF related to the DM (for ρ), from 3.34-4.04 vs 4.13-4.56 (for λ), from 7.46-8.73 vs 12.64-14.02 (for $\rho.C_p$).

For the MBVs, WF mix showed a quite uniform distribution, but with a frequency twice greater at the lowest bin than for the other bins. That was certainly due to the limited number of tests. However the variability ranges of the DMs still follow the experimental ones: comparing to Ha-1%, the same range ratio of CV was found (9.78 vs 5.66 for CVe and 9.78-10.04 vs 5.94-6.77 for CVm). Almost all mixes showed quite the same modal value except for Ha-3% which have a lower value around 1.6 g/m².%RH. That shows that an increase from 1% to 3% FC does not greatly change the exchange capacity from a deterministic point. Liuzzi et al. [68] find the same also a very low increase of MBV from 1.70 to 1.73 from 4% to 12% fibre content with olive fibres. The variability of MBV is therefore an interesting point of study of cob material for an intrinsic effect of fibres.

Sorption isotherms water contents p-values barely reach 5% from one mix to another. Nevertheless, we found very reliable values of CVs. The plotted PDFs include the effects of the specimen size, protocol and inter-laboratory variability. For so, there was no correlation between the spreads of water content at different RH load on the PDF for each case, taken individually. In fact, the cases combination tend to increase the variability at intermediate RH loads (33% - 86%) as water contents values led to two easily identifiable batches. It has been globally noticed higher spreads on the desorption phase than on the adsorption phase, especially at 55% RH load.

Globally compared to experimental values of CVs (CVe), a good consistency of distributions spreads with the variability ranges computed was found for each property. For WF mix, a low difference of CV (around 1%) was found, the same as for λ, MBVs and sorptions isotherms water content. For Ha-1% and He-1% mixes, there was a significant difference of CVs using the Lognormal distribution concerning $\rho.C_p$ (21.69% for Ha-1% and 6.66% for He-1%). *DM parameters can be found in appendix A*.

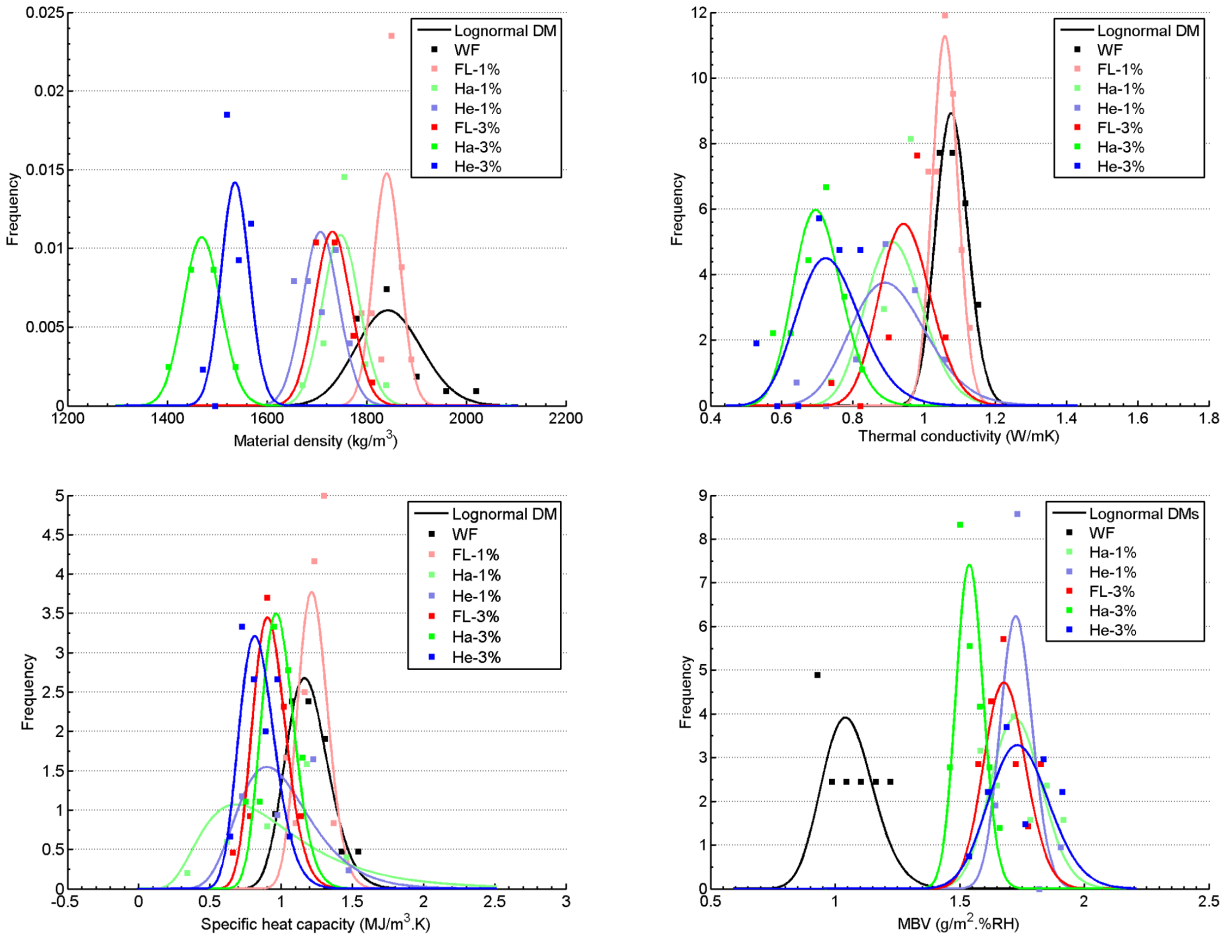

Figure 16: PDF of the material properties (density, thermal conductivity, specific heat capacity, water-vapour permeability and MBV) calculated for each formulation - markers are frequencies related the bin-clustering for each mixture (by colour) while continuous curves are least-square adaptation of a lognormal law. FL-1% data were too few to plot a PDF for MBV property.

Table 8: Statistical parameters of mixes properties. m: expectation, s: standard deviation, CVm: DM CV, CVe: experimental CV

		WF		FL-1%		Ha-1%		He-1%		FL-3%		Ha-3%		He-3%	
		m	s	m	s	m	s	m	s	m	s	m	s	m	s
ρ (kg/m^3)	Normal law	1846	67	1841	27	1749	37	1709	36	1733	36	1471	37	1537	28
	Lognormal law	1846	66	1841	27	1749	37	1709	36	1733	36	1471	37	1537	28
	Weibull law	1840	89	1840	30	1745	49	1707	45	1729	47	1470	39	1536	30
λ (W/mK)	Normal law	1.08	0.04	1.06	0.04	0.92	0.08	0.91	0.10	0.95	0.07	0.70	0.07	0.74	0.08
	Lognormal law	1.08	0.04	1.06	0.04	0.92	0.08	0.91	0.11	0.95	0.07	0.70	0.07	0.74	0.09
	Weibull law	1.08	0.05	1.06	0.04	0.92	0.06	0.91	0.09	0.95	0.06	0.70	0.07	0.74	0.07
$\rho.C_p$ (MJ/m^3.K)	Normal law	1.19	0.15	1.23	0.10	0.95	0.34	1.00	0.27	0.93	0.12	0.98	0.11	0.84	0.13
	Lognormal law	1.19	0.15	1.23	0.11	0.97	0.56	1.01	0.29	0.93	0.12	0.99	0.12	0.84	0.13
	Weibull law	1.19	0.17	1.23	0.09	0.95	0.32	1.01	0.26	0.92	0.13	0.99	0.11	0.84	0.13
k_m (10^{-12} kg/msPa)	Normal law	8.77	0.98	8.65	3.08	9.66	3.48	8.65	3.08	64.80	17.30	8.60	4.49	8.94	1.65
	Lognormal law	8.78	1.00	8.75	3.76	9.78	4.17	8.75	3.76	65.10	18.70	15.20	96.8	8.96	1.73
	Weibull law	8.76	1.01	8.66	2.92	9.68	3.27	8.66	2.92	64.80	17.10	8.31	5.34	8.96	1.59
MBV (g/m².%RH)	Normal law	1.06	0.10	-	-	1.73	0.10	1.73	0.07	1.68	0.09	1.54	0.05	1.74	0.12
	Lognormal law	1.06	0.10	-	-	1.73	0.10	1.73	0.06	1.68	0.08	1.54	0.05	1.74	0.12
	Weibull law	1.05	0.11	-	-	1.73	0.12	1.72	0.10	1.68	0.10	1.54	0.07	1.74	0.13
		WF		FL-1%		Ha-1%		He-1%		FL-3%		Ha-3%		He-3%	
		CVm	CVe	CVm	CVe	CVm	CVe	CVm	CVe	CVm	CVe	CVm	CVe	CVm	CVe
ρ (kg/m^3)	Normal law	3.62		1.46		2.11		2.12		2.09		2.52		1.82	
	Lognormal law	3.57	2.96	1.47	0.94	2.11	1.17	2.12	2.13	2.08	2.09	2.54	2.51	1.83	1.83
	Weibull law	4.85		1.62		2.80		2.61		2.74		2.64		1.98	
λ (W/mK)	Normal law	4.13		3.34		8.18		10.88		7.20		9.38		11.08	
	Lognormal law	4.15	3.79	3.34	2.88	8.78	7.71	11.99	10.03	7.64	7	9.63	8.07	12.30	10.88
	Weibull law	4.56		4.04		6.65		10.03		6.73		9.85		8.78	
$\rho.C_p$ (MJ/m^3.K)	Normal law	12.64		8.31		36.19		26.66		12.58		11.35		14.97	
	Lognormal law	12.86	12.64	8.73	8.31	57.80	36.19	29.24	26.66	12.84	12.58	11.86	11.35	15.33	14.97
	Weibull law	14.02		7.46		33.32		25.73		13.79		11.16		15.44	
k_m (kg/msPa)	Normal law	11.13		35.66		36.02		35.66		26.71		52.19		18.49	
	Lognormal law	11.43	11.71	42.93	35.66	42.68	36.02	42.93	37.09	28.69	26.71	637.40	52.19	19.28	18.49
	Weibull law	11.53		33.75		33.82		33.75		26.43		64.18		17.74	
MBV (g/m².%RH)	Normal law	9.78		-		5.96		3.82		5.08		3.52		6.99	
	Lognormal law	9.81	9.78	-	5.73	5.94	5.66	3.71	6.51	5.04	5.08	3.50	3.52	7.02	6.99
	Weibull law	10.04		-		6.77		5.84		6.01		4.40		7.65	

Table 9: Statistical parameters of sorption isotherms for various water contents. m: expectation, s: standard deviation, CVm: DM CV, CVe: experimental CV

		WF		FL-1%		Ha-1%		He-1%		Ha-3%	
		m	s	m	s	m	s	m	s	m	s
12%	Normal law	0.62	0.25	0.74	0.22	0.71	0.17	0.85	36.26	0.95	0.63
	Lognormal law	0.62	0.25	0.74	0.23	0.71	0.17	0.85	36.15	0.96	0.87
	Weibull law	0.62	0.25	0.74	0.22	0.71	0.18	0.85	44.56	0.96	0.58
33%	Normal law	0.95	0.28	1.17	0.26	1.16	0.21	1.45	0.27	1.28	0.64
	Lognormal law	0.95	0.28	1.17	0.27	1.16	0.21	1.45	0.28	1.29	0.74
	Weibull law	0.95	0.29	1.17	0.27	1.15	0.22	1.45	0.26	1.29	0.60
55%	Normal law	1.30	0.29	1.58	0.24	1.61	0.23	1.99	0.24	1.64	0.59
	Lognormal law	1.30	0.29	1.59	0.24	1.61	0.23	2.00	0.24	1.64	0.63
	Weibull law	1.30	0.32	1.58	0.26	1.61	0.24	2.00	0.24	1.65	0.57
75%	Normal law	1.76	0.22	2.20	0.16	2.23	0.18	2.75	0.16	2.11	0.41
	Lognormal law	1.76	0.22	2.20	0.16	2.23	0.18	2.75	0.16	2.11	0.41
	Weibull law	1.75	0.25	2.20	0.17	2.22	0.20	2.75	0.15	2.11	0.42
90%	Normal law	2.17	0.20	2.75	0.27	2.78	0.25	3.42	0.26	2.67	0.19
	Lognormal law	2.17	0.21	2.75	0.27	2.78	0.26	3.42	0.27	2.67	0.19
	Weibull law	2.17	0.20	2.73	0.32	2.78	0.22	3.42	0.28	2.67	0.20
		WF		FL-1%		Ha-1%		He-1%		Ha-3%	
		CVm	CVe	CVm	CVe	CVm	CVe	CVm	CVe	CVm	CVe
12%	Normal law	40.54		24.29		29.93		22.19		66.03	
	Lognormal law	40.48	40.54	24.25	24.29	31.26	29.93	22.84	36.26	90.18	66.03
	Weibull law	40.32		25.30		29.78		22.82		60.72	
33%	Normal law	29.26		17.98		22.32		18.32		49.62	
	Lognormal law	29.27	29.26	18.15	17.98	22.86	22.32	19.03	18.32	57.21	49.62
	Weibull law	30.64		18.88		22.76		18.14		46.21	
55%	Normal law	22.59		14.17		15.15		11.98		36.09	
	Lognormal law	22.43	22.59	14.24	14.17	15.21	15.15	12.27	11.98	38.06	36.09
	Weibull law	24.58		14.89		16.13		11.94		34.68	
75%	Normal law	12.52		7.87		7.34		5.87		19.52	
	Lognormal law	12.58	12.52	7.86	7.87	7.43	7.34	5.98	5.87	19.55	19.52
	Weibull law	14.44		9.01		7.73		5.46		20.06	
90%	Normal law	9.25		8.85		9.92		7.72		7.04	
	Lognormal law	9.45	9.25	9.25	8.85	9.86	9.92	7.82	7.72	7.08	7.04
	Weibull law	9.26		8.08		11.78		8.19		7.39	

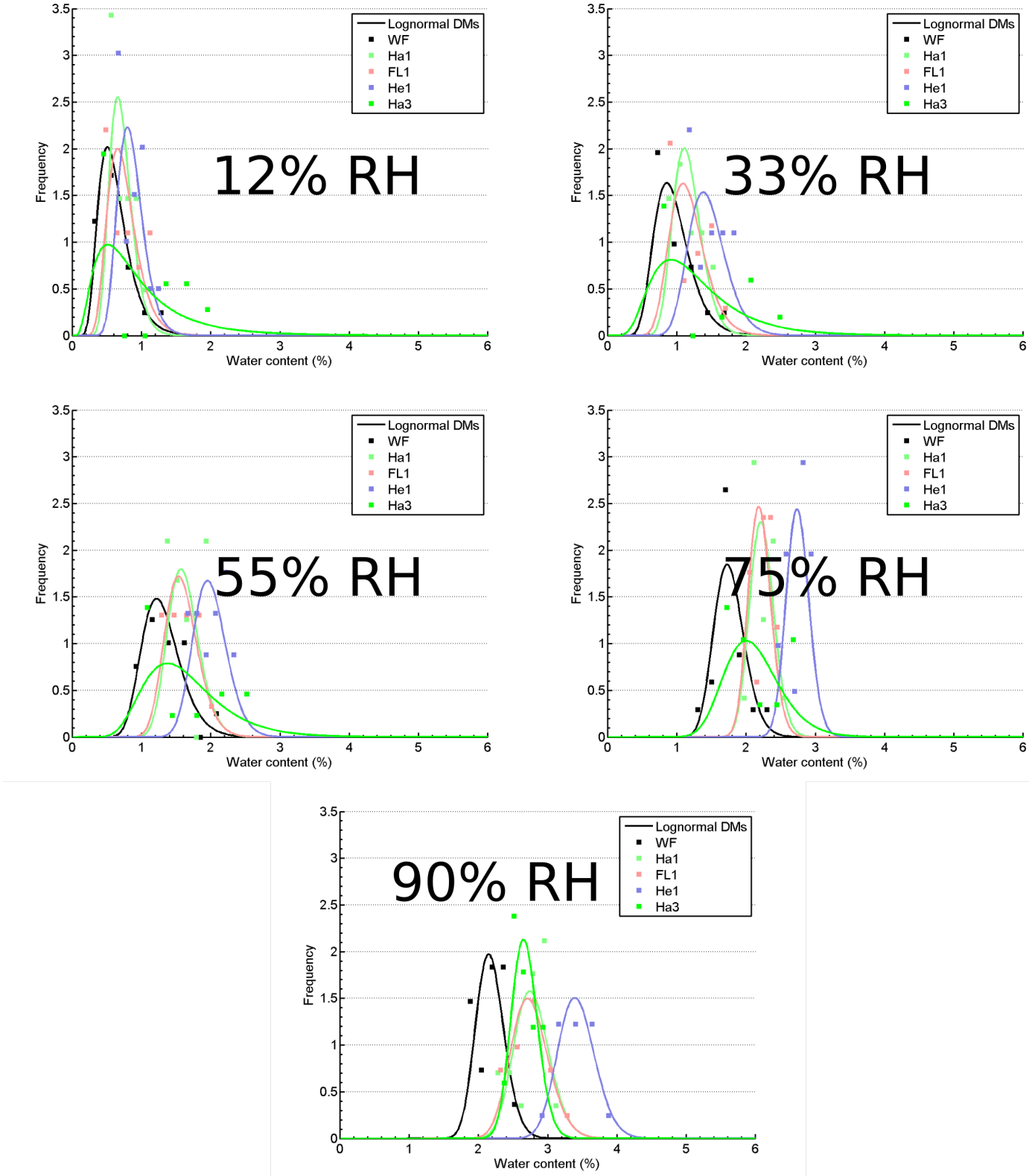

Figure 17: Probability density functions corresponding to the adsorption phase calculated for each RH load and for each formulation - markers are frequencies related the bin-clustering for each mixture (by colour) while continuous curves are least-square adaptation of a lognormal law

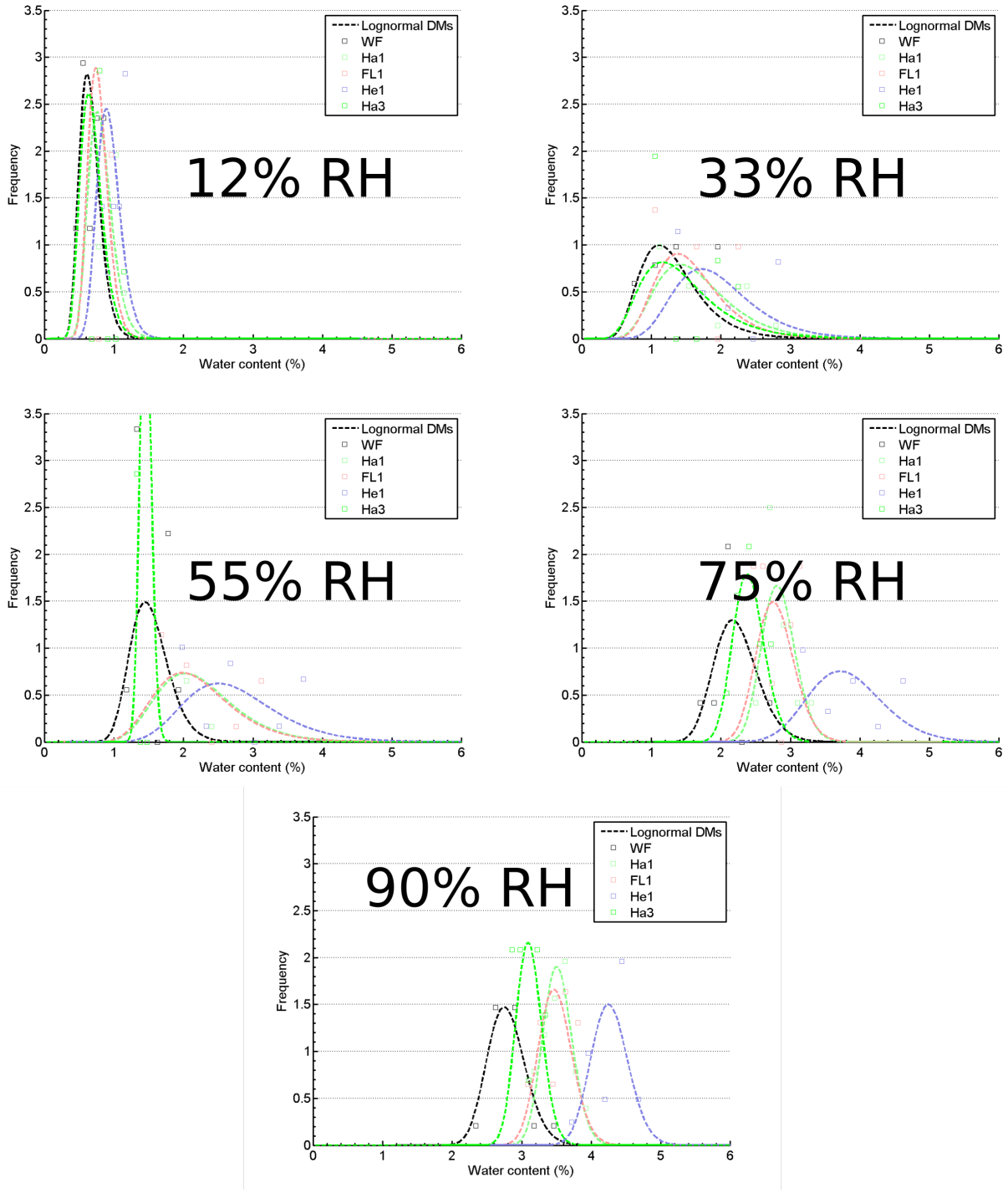

Figure 18: Probability density functions corresponding to the desorption phase calculated for each RH load and for each formulation - markers are frequencies related the bin-clustering for each mixture (by colour) while continuous curves are least-square adaptation of a lognormal law

4.2. Discussion on the evolution laws of the variability of cob materials properties

The figure 19 displays the evolution of the variability of material properties according to the content of plants add-ons in the mixtures. It shows our study data combined to Barnaure et al data [54] and an evolution trend. Barnaure et al. have studied the variability for an unfibred mix and a fibred mix with 8% fibre content (7% of hemp shives and 1% of reed), with a water content in specimens around 3% by mean. According to the property and the fibre specie, the material variability should progress differently, but we assume hemp fibres as prevailing in the mix.

For Density (figure 19a), there was a FC for which the cob composites showed a minimum of variability

(FC^{min}), whatever the fibre specie. FC^{min} was not more than 1% whatever the fibre specie. The minimum of variability level was not the same according to the plant fibre as we can distinctly see between hemp composite and Flax composite. According to the observed trend, there should be a large variability at higher FC. This trend is related to the uncontrolled compaction during molding, as it is found in literature low standard deviations with increasing fibre content inside mixtures, even in the light materials [7, 36, 69].

For thermal conductivity (figure 19b), the variability trend showed a highest value FC^{max} and then decreased up to a residual variability FC^{res}. FC^{max} value is found not more than 1% for Hay stalks and Flax composites, while it is found more than 3% for Hemp composites. Water content inside the material have a great influence on FC limits as water change heat diffusion paths and kinetics, and thus thermal properties. Therfore, FC^{max} of λ for Barnaure et al [54] measurements is lower than 6%.

For specific heat capacity, we noticed two trends according to the fibre specie. For plant bark of stem represented by hemp shives and hay stalks in this study, we notice an increase of the variability until a FC^{max} and then a reduction until a residual FC^{res} (trend1). That could account for the high spread of plants fibre at low FC. At higher FC, the material increasingly becomes homogeneous. This trend is confirmed, thanks to data provided by Barnaure et al [54]. For plant fibres represented by flax yarns in our study, there is an attenuation of $\rho.C_p$ up to FC^{min} and then an increase to a residual FC^{res} (trend2). The increase of the variability is due to an increase of fibres batches inside the specimens due to their low diameter.

For water vapour permeability (figure 19d), the trend is the same as λ property. Indeed, water vapour diffusion mean free path variability decrease when material homogeneity increase (high FC). Thus FC^{max} is not more than 1% FC for Hemp and Flax mixes (data here are those for SSS solution - the numbers of specimens are not the same). This value is found more than 3% using Hay stalks composites.

Do the variabilities of λ, $\rho.C_p$, k_m become negligible with lightweight cob composites using plant barks or stems as fibre? one should notice from one way that there is no way to reach high FC and retain the plastic state of earth composite. Moreover, Hamard et al [70] reviewed a FC ranging from 0.3-2% on real cob buildings. FC^{res} is not therefore a required parameter from a practical point of view.

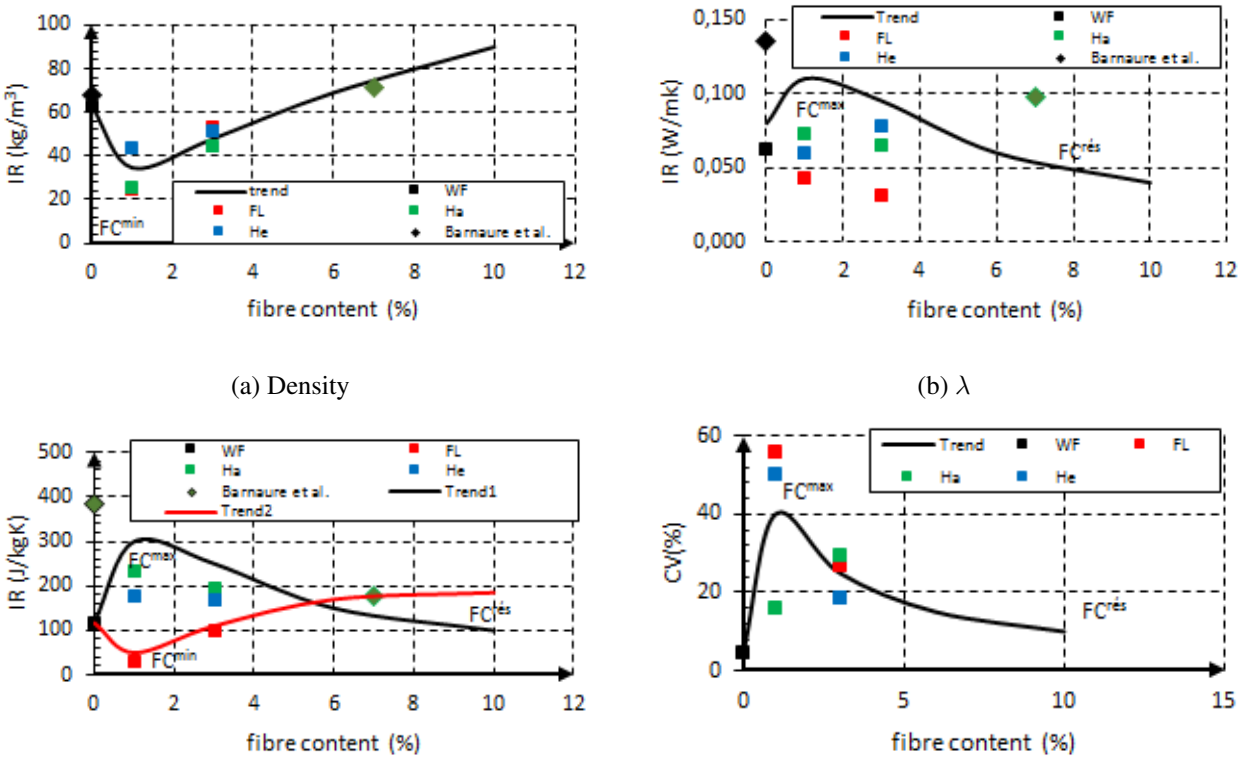

(a) Density

(b) λ

(c) $\rho.C_p$

(d) k_m

Figure 19: Evolution of the variability of material properties

5. Conclusion

Nowadays, earth construction knows an increasing interest because of the exhausting of natural resources and of the need to reinvent the construction sector, by promoting new construction techniques and materials able to address the crucial issue of global climate change. However, the hygrothermal behaviour of earthen materials is not well taken into account by engineers in charge of the buildings energy performance optimisation. This is due to the fact that moisture transfer is generally neglected by the design software, but also to a lack of knowledge about the hygrothermal properties of these materials. Indeed, the values of these properties are not always available and where available, differences can be observed between the databases. Therefore, there is a need to better quantify the values of these various properties as well as the associated variability.

In this paper, an extensive analysis of the experimental values of the heat and water vapour transfer parameters of different formulations of earthen composites was performed. The aim was to identify the average value for each parameter but also to identify the variability induced by the material heterogeneity or the uncertainty of the measurement techniques. The aim was also to determine the experimental PDFs for each parameter and each formulation and to adapt mathematical models able to give estimates of the mean, standard deviation and coefficient of variation. The values of these parameters were compared to experimental mean and CVs. The following results have been obtained:

- the density and the thermal conductivity for different fibre species and fibre content showed a linear correlation.
- The variability of the dry bulk density of cob materials increases with fiber content.
- The variability of the water vapour permeability of mixes was performed using dry cup tests and the proUmid device. It was found to be sensitive to the specimen representative elementary volume as the Gravitest method shows a CV 12% greater than the dry cup test method by mean. However, the addition of plant fibres obviously increases the variability, with a CV ranging from 18%-50% in fibred composites while it is 4.49% for WF mix, using manual DCT.
- The water contents of sorption isotherms exhibit higher variations at low humidity loads. The variability was more pronounced with hydrophobic fibred mixes (He-1% and Ha-1%) than with FL-1% mix. The specimen representation was also a determinant factor of the variability as sorption mean value and variability were higher at intermediate relative humidity loads with Saturated Salt Solutions method than ProUmid one.
- PDFs of the various properties have been provided for stochastic analysis purposes. After a statistical analysis on the bins number using p-value as criteria, there was a weak difference from one PDF to another for the considered models. Statistical indicators obtained from the models were in accordance with experimental distributions. Indeed, for water vapour permeability and sorption isotherms of some mixes, there was some relevance between water content spread of pdf and the experimental coefficient of variation (if considering batches separately).
- Finally, the evolution trends of the variability of some material properties were identified. The variability of thermal conductivity and the water vapour permeability follows the same law: an increase at the low fibre contents (FCs) and decrease for high FCs. The high variability of the latter is due to material heterogeneity. The variability of SHC depend on the plant specie - the variability with plants cells composites follows a decreasing trend at lower FC and then an increasing trend, inversely to plants barks/stems composites.

A further work is to improve of the cob representativeness, notably on characteristics such as the vegetal fibres lengths, the number of manufacturers, the vernacular wall mounting, the man-made feet mixing, the water content [71] etc. Moreover, there is a need to provide tests on other fibres species and refine the evolution trends of the variability (numerical trend) and thus improve decision-makers variability (designers, lawmakers, etc.). Finally, the variation range and the probability density function of the properties could be used either to find the reliability on energy estimation of cob buildings or a representative value of energy consumption (by using modal values of PDFs).

6. Acknowledgements

Authors thank the French Agency of Environment and Energy Management Agency (ADEME) and Pays de la Loire Region (in France) for supporting this work. Special thanks to Palladio foundation too, for material funding. Thanks to the LASIE laboratory (La Rochelle) which has enrich the database by performing water vapour permeability tests with Gravitest and water-vapor sorption test with ProUmid tests. Special thanks too to Fan YANG and Léo LAVENAN, 4th year engineer student and Master 2 student who helped during performing some reproductibility tests of hotdisk and MBV tests. Thanks to Mircea Barnaure, for providing his data for a better interpretation of evolution laws of the variability for cob materials properties.

References

[1] T. R. Karl, R. W. Knight, and B. Baker, "The record breaking global temperatures of 1997 and 1998: Evidence for an increase in the rate of global warming?," Geophysical Research Letters, vol. 27, no. 5, pp. 719–722, 2000.

[2] I. P. O. C. Change, "ipcc_wg_i_1992_suppl_report_full_report.pdf," tech. rep., 1992.

[3] U. N. Environment, "2019 Global Status Report for Buildings and Construction Sector," Nov. 2019. Section: publications.

[4] M.-S. Seo, T. Kim, G. Hong, and H. Kim, "On-Site Measurements of CO2 Emissions during the Construction Phase of a Building Complex," Energies, vol. 9, p. 599, Aug. 2016.

[5] J. Lee, S. Tae, and R. Kim, "A Study on the Analysis of CO2 Emissions of Apartment Housing in the Construction Process," Sustainability, vol. 10, p. 365, Feb. 2018.

[6] A. Laborel-Préneron, J. E. Aubert, C. Magniont, C. Tribout, and A. Bertron, "Plant aggregates and fibers in earth construction materials: A review," Construction and Building Materials, vol. 111, pp. 719–734, May 2016.

[7] D. Medjelekh, L. Ulmet, F. Gouny, F. Fouchal, B. Nait-Ali, P. Maillard, and F. Dubois, "Characterization of the coupled hygrothermal behavior of unfired clay masonries: Numerical and experimental aspects," Building and Environment, vol. 110, pp. 89–103, Dec. 2016.

[8] H. Hugo, H. Guillaud, and CRAterre, Traité de construction en terre. Editions Paranthèses, 2006.

[9] H. Niroumand, M. F. M. Zain, and M. Jamil, "Various Types of Earth Buildings," Procedia - Social and Behavioral Sciences, vol. 89, pp. 226–230, Oct. 2013.

[10] F. Collet, L. Serres, J. Miriel, and M. Bart, "Study of thermal behaviour of clay wall facing south," Building and Environment, vol. 41, pp. 307–315, Mar. 2006.

[11] M. de la transition écologique et solidaire, ed., Guide des bonnes pratiques de la construction en terre crue. 2018.

[12] G. B. Baescher and J. T. Christian, "Spatial variability and geotechnical reliability," in Reliability-Based Design in Geotechnical Engineering: Computations and Applications, pp. 76 – 133, 2008.

[13] K.-K. Phoon and F. H. Kulhawy, "Characterization of geotechnical variability," Canadian Geotechnical Journal, vol. 36, pp. 612–624, Nov. 1999.

[14] "NF ISO 21748 - Juillet 2017," 2017.

[15] "NF ISO 5725-4," 2020.

[16] K.-K. Phoon and F. H. Kulhawy, "Evaluation of geotechnical property variability," Canadian Geotechnical Journal, vol. 36, pp. 625–639, Nov. 1999.

[17] W. A. Shewhart and W. E. Deming, Statistical Method from the Viewpoint of Quality Control. Courier Corporation, Jan. 1986. Google-Books-ID: ALGbNNMdnHkC.

[18] T. Vinceslas, Caractérisation d'éco-matériaux terre-chanvre en prenant en compte la variabilité des ressources disponibles localement. PhD thesis, Université Bretagne Loire, Lorient, 2019.

[19] J.-E. Aubert, "Caractérisation des briques de terre crue de Midi-Pyrénées," tech. rep., Laboratoire de Recherche en Architecture (LRA) - ENSA Toulouse, Apr. 2013.

[20] C. Niyigena, S. Amziane, A. Chateauneuf, L. Arnaud, L. Bessette, F. Collet, C. Lanos, G. Escadeillas, M. Lawrence, C. Magniont, S. Marceau, S. Pavia, U. Peter, V. Picandet, M. Sonebi, and P. Walker, "Variability of the mechanical properties of hemp concrete," Materials Today Communications, vol. 7, pp. 122–133, June 2016.

[21] M. Hall and D. Allinson, "Assessing the effects of soil grading on the moisture content-dependent thermal conductivity of stabilised rammed earth materials," Applied Thermal Engineering, vol. 29, pp. 740–747, Mar. 2009.

[22] M. Hall and D. Allinson, "Analysis of the hygrothermal functional properties of stabilised rammed earth materials," Building and Environment, vol. 44, pp. 1935–1942, Sept. 2009.

[23] T. Ashour, H. Georg, and W. Wu, "An experimental investigation on equilibrium moisture content of earth plaster with natural reinforcement fibres for straw bale buildings," Applied Thermal Engineering, vol. 31, pp. 293–303, Feb. 2011.

[24] T. Ashour, H. Wieland, H. Georg, F.-J. Bockisch, and W. Wu, "The influence of natural reinforcement fibres on insulation values of earth plaster for straw bale buildings," Materials & Design, vol. 31, pp. 4676–4685, Dec. 2010.

[25] S. Guihéneuf, D. Rangeard, A. Perrot, T. Cusin, F. Collet, and S. Prétot, "Effect of bio-stabilizers on capillary absorption and water vapour transfer into raw earth," Materials and Structures, vol. 53, p. 138, Nov. 2020.

[26] O. López, I. Torres, A. S. Guimarães, J. M. P. Q. Delgado, and V. P. de Freitas, "Inter-laboratory variability results of porous building materials hygrothermal properties," Construction and Building Materials, vol. 156, pp. 412–423, Dec. 2017.

[27] F. El Fgaier, Z. Lafhaj, E. Antczak, and C. Chapiseau, "Dynamic thermal performance of three types of unfired earth bricks," Applied Thermal Engineering, vol. 93, pp. 377–383, Jan. 2016.

[28] M. Barnaure, S. Bonnet, and P. Poullain, "Earth buildings with local materials: Assessing the variability of properties measured using non-destructive methods," Construction and Building Materials, vol. 281, p. 122613, 2021.

[29] A. B. Laibi, P. Poullain, N. Leklou, M. Gomina, and D. K. C. Sohounhloué, "Influence of the kenaf fiber length on the mechanical and thermal properties of Compressed Earth Blocks (CEB)," KSCE Journal of Civil Engineering, vol. 22, pp. 785–793, Feb. 2018.

[30] P. Maillard and J. E. Aubert, "Effects of the anisotropy of extruded earth bricks on their hygrothermal properties," Construction and Building Materials, vol. 63, pp. 56–61, July 2014.

[31] H. Cagnon, J. E. Aubert, M. Coutand, and C. Magniont, "Hygrothermal properties of earth bricks," Energy and Buildings, vol. 80, pp. 208–217, Sept. 2014.

[32] O. Ines, P. Poullain, A.-N. Leklou, and A. Caucheteux, "Sensitivity analysis of the Künzel model: application to the study of the hygrothermal transfer in a tuffeau wall," in Heat Transfer XIII:Simulation and Experiments in Heat and Mass Transfer, Heat Transfer XIII:Simulation and Experiments in Heat and Mass Transfer, (La Corogne, Spain), WIT Press, 2014.

[33] R. Bui, J. Goffart, F. McGregor, M. Woloszyn, A. Fabbri, and A.-C. Grillet, "Uncertainty and sensitivity analysis applied to a rammed earth wall: evaluation of the discrepancies between experimental and numerical data," E3S Web of Conferences, vol. 172, p. 17004, 2020.

[34] Andrianandraina, P. Poullain, B. Cazacliu, and A. Ventura, "SENSITIVITY ANALYSIS OF PARAMETERS INFLUENCING BUILDING HEATING ENERGY CONSUMPTION USING HEMP-LIME MATERIAL," p. 8, 2015.

[35] C. Feng, H. Janssen, Y. Feng, and Q. Meng, "Hygric properties of porous building materials: Analysis of measurement repeatability and reproducibility," Building and Environment, vol. 85, pp. 160–172, Feb. 2015.

[36] M. Labat, C. Magniont, N. Oudhof, and J.-E. Aubert, "From the experimental characterization of the hygrothermal properties of straw-clay mixtures to the numerical assessment of their buffering potential," Building and Environment, vol. 97, pp. 69–81, Feb. 2016.

[37] R. M. Gandia, F. C. Gomes, A. A. R. Corrêa, M. C. Rodrigues, and R. F. Mendes, "Physical, mechanical and thermal behavior of adobe stabilized with glass fiber reinforced polymer waste," Construction and Building Materials, vol. 222, pp. 168–182, Oct. 2019.

[38] "NF ISO 17892-4," 2018.

[39] A. R. de Forges, C. Feller, and M. Jamagne, "Perdus dans le triangle des textures," Etude et Gestion des Sols, p. 16, 2008.

[40] F. Rojat, E. Hamard, A. Fabbri, B. CARNUS, and F. McGregor, "Towards an easy decision tool to assess soil suitability for earth building," Construction and Building Materials, vol. 257, p. 28 p., Jan. 2020.

[41] E. Hamard, B. Lemercier, B. Cazacliu, A. Razakamanantsoa, and J.-C. Morel, "A new methodology to identify and quantify material resource at a large scale for earth construction – Application to cob in Brittany," Construction and Building Materials, vol. 170, pp. 485–497, May 2018.

[42] "NF EN ISO 17892-12 reconnaissance et essais géotechniques - essais de laboratoire sur les sols - partie 12 : détermination des limites de liquidité et de plasticité," 2018.

[43] "NF P11-300," 1992.

[44] "NF en 933-9 +a1," 2013.

[45] V. Dakshanamurthy and V. Raman, "A Simple Method of Identifying an Expansive Soil," Soils and Foundations, vol. 13, pp. 97–104, Mar. 1973.

[46] M. Türköz and H. Tosun, "The use of methylene blue test for predicting swell parameters of natural clay soils," Sci. Res. Essays, p. 13, Apr. 2011.

[47] P. Glé, T. Lecompte, A. Hellouin de Ménibus, H. Lenormand, S. Arufe, C. Chateau, V. Fierro, and A. Celzard, "Densities of hemp shiv for building: From multiscale characterisation to application," Industrial Crops and Products, vol. 164, p. 113390, June 2021.

[48] M. Viel, F. Collet, S. Pretot, and C. Lanos, "Hemp-Straw Composites: Gluing Study and Multi-Physical Characterizations," Materials, vol. 12, p. 1199, Apr. 2019.

[49] H. Yang, Study of a unidirectional flax reinforcement for biobased composite. These de doctorat, CAEN Normandie, July 2017.

[50] R. Olivito, O. Cevallos, and A. Carrozzini, "Development of durable cementitious composites using sisal and flax fabrics for reinforcement of masonry structures," Materials & Design, vol. 57, pp. 258–268, May 2014.

[51] C. Baley, "Analysis of the flax fibres tensile behaviour and analysis of the tensile stiffness increase," Composites Part A: Applied Science and Manufacturing, vol. 33, pp. 939–948, July 2002.

[52] A. Lisowski, P. Matkowski, M. Dabrowska, M. Piatek, A. Świetochowski, J. Klonowski, L. Mieszkalski, and V. Reshetiuk, "Particle Size Distribution and Physicochemical Properties of Pellets Made of Straw, Hay, and Their Blends," Waste and Biomass Valorization, vol. 11, pp. 63–75, Jan. 2020.

[53] M. L. Guen, "La boîte à moustaches de TUKEY, un outil pour initier à la Statistique," p. 16, June 2008.

[54] M. Barnaure, B. Stéphanie, and P. Poullain, "Earth buildings with local materials : assessing the variability of properties measured using non-destructive methods," Construction and Building Materials, January 2021.

[55] E. Quagliarini, A. Stazi, E. Pasqualini, and E. Fratalocchi, "Cob Construction in Italy: Some Lessons from the Past," Sustainability, vol. 2, pp. 3291–3308, Oct. 2010.

[56] T. Ashour and W. Wu, "An experimental study on shrinkage of earth plaster with natural fibres for straw bale buildings," International Journal of Sustainable Engineering, vol. 3, pp. 299–304, Dec. 2010.

[57] S. Sangma and D. D. Tripura, "Experimental study on shrinkage behaviour of earth walling materials with fibers and stabilizer for cob building," Construction and Building Materials, vol. 256, p. 119449, Sept. 2020.

[58] M. Gustavsson, E. Karawacki, and S. E. Gustafsson, "Thermal conductivity, thermal diffusivity, and specific heat of thin samples from transient measurements with hot disk sensors," Review of Scientific Instruments, vol. 65, pp. 3856–3859, Dec. 1994.

[59] T. Colinart, M. Pajeot, T. Vinceslas, A. Hellouin De Menibus, and T. Lecompte, "Thermal conductivity of biobased insulation building materials measured by hot disk: Possibilities and recommendation," Journal of Building Engineering, vol. 43, p. 102858, Nov. 2021.

[60] A. A. Trofimov, J. Atchley, S. S. Shrestha, A. O. Desjarlais, and H. Wang, "Evaluation of measuring thermal conductivity of isotropic and anisotropic thermally insulating materials by transient plane source (Hot Disk) technique," Journal of Porous Materials, vol. 27, pp. 1791–1800, Dec. 2020.

[61] "NF EN ISO 12572," Oct. 2016.

[62] F. Benmahiddine, F. Bennai, R. Cherif, R. Belarbi, A. Tahakourt, and K. Abahri, "Experimental investigation on the influence of immersion/drying cycles on the hygrothermal and mechanical properties of hemp concrete," Journal of Building Engineering, vol. 32, p. 101758, Nov. 2020.

[63] "Nf en 12571," November 2021.

[64] C. Rode, R. H. Peuhkuri, K. K. Hansen, B. Time, K. Svennberg, J. Arfvidsson, and T. Ojanen, "Nordtest project on moisture buffer value of materials," Materials, vol. 12, p. 7, 2005.

[65] L. Ba, I. El Abbassi, T.-T. Ngo, P. Pliya, C. S. E. Kane, A.-M. Darcherif, and M. Ndongo, "Experimental investigation of thermal and mechanical properties of clay reinforced with typha australis: Influence of length and percentage of fibers," Waste and Biomass Valorization, vol. 12, no. 5, pp. 2723–2737, 2021.

[66] Y. Millogo, J.-C. Morel, J.-E. Aubert, and K. Ghavami, "Experimental analysis of pressed adobe blocks reinforced with hibiscus cannabinus fibers," Construction and Building Materials, vol. 52, pp. 71–78, 2014.

[67] J.-P. Laurent, Contribution à la caractérisation thermique des milieux poreux granulaires: optimisation d'outils de mesure" in-situ" des paramètres thermiques, application à l'étude des propriétés thermiques du matériau terre. PhD thesis, Grenoble INPG, 1986.

[68] S. Liuzzi, C. Rubino, P. Stefanizzi, A. Petrella, A. Boghetich, C. Casavola, and G. Pappalettera, "Hygrothermal properties of clayey plasters with olive fibers," Construction and Building Materials, vol. 158, pp. 24–32, Jan. 2018.

[69] E. B. Ojo, K. O. Bello, K. Mustapha, R. S. Teixeira, S. F. Santos, and H. Savastano, "Effects of fibre reinforcements on properties of extruded alkali activated earthen building materials," Construction and Building Materials, vol. 227, p. 116778, Dec. 2019.

[70] E. Hamard, B. Cazacliu, A. Razakamanantsoa, and J.-C. Morel, "Cob, a vernacular earth construction process in the context of modern sustainable building," Building and Environment, vol. 106, pp. 103–119, 2016.

[71] R. Allam, I. Nabil, R. Belarbi, M. El-Meligy, and A. Altahrany, "Hygrothermal behavior for a clay brick wall," Heat and Mass Transfer, vol. 54, June 2018.

Appendix

A. probability density function parameters of materials properties

		WF		FL-1%		Ha-1%		He-1%		FL-3%		Ha-3%		He-3%	
		$\mu\|\lambda$	$\sigma\|k$	$\mu\|\lambda$	$\sigma\|k$	$\mu\|\lambda$	$\sigma\|k$	$\mu\|\lambda$	$\sigma\|k$	$\mu\|\lambda$	$\sigma\|k$	$\mu\|\lambda$	$\sigma\|k$	$\mu\|\lambda$	$\sigma\|k$
ρ (kg/m^3)	Normal law	1846.28	66.79	1841.18	26.94	1748.94	36.82	1708.72	36.26	1732.67	36.19	1470.67	37.08	1536.78	28.04
	Lognormal law	0.80	7.52	0.31	7.52	0.31	7.47	0.79	7.44	0.50	7.46	0.67	7.29	0.70	7.34
	Weibull law	1879.60	25.74	1853.52	78.49	1766.85	45.05	1726.48	48.40	1750.46	46.07	1487.58	47.89	1549.88	64.16
λ (W/mK)	Normal law	1.08	0.04	1.06	0.04	0.92	0.08	0.91	0.10	0.95	0.07	0.70	0.07	0.74	0.08
	Lognormal law	0.66	0.07	0.97	0.06	0.11	-0.09	0.16	-0.10	0.01	-0.05	0.29	-0.35	0.05	-0.31
	Weibull law	1.10	27.42	1.08	31.03	0.95	18.60	0.95	12.12	0.98	18.35	0.73	12.35	0.77	13.92
$\rho.C_p$ (MJ/m^3.K)	Normal law	1.19	0.15	1.23	0.10	0.95	0.34	1.00	0.27	0.93	0.12	0.98	0.11	0.84	0.13
	Lognormal law	0.79	0.17	0.31	0.20	0.35	-0.14	0.33	-0.03	0.93	-0.08	0.47	-0.02	0.44	-0.18
	Weibull law	1.26	8.50	1.27	16.50	1.05	3.31	1.10	4.40	0.98	8.65	1.03	10.82	0.90	7.67
MBV (g/m².%RH)	Normal law	1.06	0.10	-	-	1.73	0.10	1.73	0.07	1.68	0.09	1.54	0.05	1.74	0.12
	Lognormal law	0.24	0.05	-	-	0.76	0.55	0.07	0.55	0.28	0.52	0.90	0.43	0.87	0.55
	Weibull law	1.10	12.10	-	-	1.78	18.25	1.76	21.27	1.72	20.66	1.57	28.44	1.80	16.08

Table A. 1: Density, thermal conductivity, specific heat capacity, Moisture buffering value distribution model parameters of mixtures.

		WF		Ha-1%		FL-1%		He-1%		Ha-3%	
		$\mu\|\lambda$	$\sigma\|k$	$\mu\|\lambda$	$\sigma\|k$	$\mu\|\lambda$	$\sigma\|k$	$\mu\|\lambda$	$\sigma\|k$	$\mu\|\lambda$	$\sigma\|k$
12%	Normal law	0.62	0.25	0.71	0.17	0.74	0.22	0.85	36.26	0.95	0.63
	Lognormal law	-0.55	0.37	-0.37	0.23	-0.34	0.29	-0.18	36.15	-0.25	0.65
	Weibull law	0.70	2.67	0.78	4.48	0.82	3.74	0.93	44.56	1.07	1.69
33%	Normal law	0.95	0.28	1.16	0.21	1.17	0.26	1.45	0.27	1.28	0.64
	Lognormal law	-0.09	0.28	0.13	0.18	0.13	0.22	0.36	0.19	0.14	0.48
	Weibull law	1.05	3.63	1.24	6.17	1.27	5.04	1.56	6.44	1.46	2.29
55%	Normal law	1.30	0.29	1.61	0.23	1.58	0.24	1.99	0.24	1.64	0.59
	Lognormal law	0.24	0.22	0.47	0.14	0.45	0.15	0.68	0.12	0.44	0.35
	Weibull law	1.42	4.63	1.71	7.97	1.69	7.31	2.10	10.08	1.84	3.16
75%	Normal law	1.76	0.22	2.23	0.18	2.20	0.16	2.75	0.16	2.11	0.41
	Lognormal law	0.56	0.12	0.80	0.08	0.79	0.07	1.01	0.06	0.73	0.19
	Weibull law	1.86	8.24	2.31	13.56	2.27	15.91	2.82	22.77	2.28	5.78
90%	Normal law	2.17	0.20	2.78	0.25	2.75	0.27	3.42	0.26	2.67	0.19
	Lognormal law	0.77	0.09	1.02	0.09	1.01	0.10	1.23	0.08	0.98	0.07
	Weibull law	2.26	13.18	2.88	15.20	2.87	10.23	3.54	14.98	2.75	16.66

Table A. 2: Distribution model parameters of adsorption isotherms of mixtures.

		WF		Ha-1%		FL-1%		He-1%		Ha-3%	
		$\mu\|\lambda$	$\sigma\|k$	$\mu\|\lambda$	$\sigma\|k$	$\mu\|\lambda$	$\sigma\|k$	$\mu\|\lambda$	$\sigma\|k$	$\mu\|\lambda$	$\sigma\|k$
12%	Normal law	0.66	0.14	0.81	0.18	0.77	0.14	0.93	36.26	0.68	0.18
	Lognormal law	-0.44	0.23	-0.23	0.21	-0.27	0.18	-0.09	36.15	-0.41	0.24
	Weibull law	0.71	5.44	0.88	5.05	0.83	7.05	1.00	44.56	0.75	3.99
33%	Normal law	1.31	0.45	1.67	0.60	1.58	0.49	1.96	0.60	1.45	0.58
	Lognormal law	0.22	0.34	0.46	0.34	0.41	0.31	0.63	0.30	0.30	0.39
	Weibull law	1.47	3.32	1.87	3.08	1.75	3.68	2.18	3.66	1.63	2.89
55%	Normal law	1.52	0.28	2.24	0.61	2.20	0.60	2.74	0.71	1.45	0.08
	Lognormal law	0.40	0.18	0.77	0.26	0.75	0.26	0.98	0.25	0.37	0.06
	Weibull law	1.63	6.28	2.47	4.07	2.42	4.12	3.01	4.26	1.49	22.34
75%	Normal law	2.23	0.31	2.83	0.25	2.79	0.27	3.82	0.54	2.40	0.23
	Lognormal law	0.79	0.14	1.04	0.09	1.02	0.10	1.33	0.14	0.87	0.09
	Weibull law	2.36	8.46	2.95	11.59	2.91	11.98	4.05	8.39	2.51	11.73
90%	Normal law	2.79	0.28	3.52	0.21	3.49	0.24	4.27	0.26	3.11	0.19
	Lognormal law	1.02	0.10	1.26	0.06	1.25	0.07	1.45	0.06	1.13	0.06
	Weibull law	2.91	10.13	3.61	19.49	3.59	18.87	4.39	19.86	3.19	19.88

Table A. 3: Distribution model parameters of desorption isotherms of mixtures.